

Aus der Anatomischen Anstalt, Lehrstuhl III
der Ludwig-Maximilians-Universität München
Vorstand: Professor Dr. med. Winfried Lange

The organization and function of medial rectus and inferior rectus non-twitch
motoneurons in the oculomotor nucleus of monkey

Dissertation

zum Erwerb des Doktorgrades der Medizin
an der Medizinischen Fakultät der
Ludwig-Maximilians-Universität zu München

vorgelegt von

Xiaofang Tang

Aus Weihai, Shandong, P. R. China

2007

Mit Genehmigung der Medizinischen Fakultät
Der Universität München

Berichterstatter: Frau Prof. Dr. Jean Büttner-Ennever

Mitberichterstatter: Prof. Dr. P. Grafe
Prof. Dr. A. Kampik

Mitbetreuung durch den
promovierten Mitarbeiter: PD Dr. rer. nat Anja Horn-Bochtler

Dekan: Prof. Dr. med. D. Reinhardt

Tag der mündlichen Prüfung: 24.05.2007

Contents

| | |
|--|----|
| Abstract | 1 |
| Zusammenfassung | 2 |
| Abbreviations | 3 |
| 1 Introduction | 5 |
| 1.1 Extraocular muscles | 5 |
| 1.1.1 Structure of extraocular muscles | 6 |
| 1.1.2 Different types of extraocular muscles fibers | 7 |
| 1.2 Motoneurons of extraocular muscles | 9 |
| 1.3 Primary function of extraocular muscles and eye movement | 11 |
| 1.4 Aim..... | 13 |
| 2 Material and Methods..... | 14 |
| 2.1 Introduction of tract-tracing methods..... | 14 |
| 2.1.1 Tracer WGA-HRP | 16 |
| 2.1.2 Tracer cholera toxin subunit B..... | 16 |
| 2.2 Injection of tracer | 16 |
| 2.3 Perfusion..... | 18 |
| 2.4 Immunocytochemical labelling..... | 18 |
| 2.4.1 WGA-HRP immunocytochemical labelling..... | 18 |
| 2.4.2 Cholera toxin subunit B immunocytochemical labelling..... | 18 |
| 2.5 Photographic software and analysis of stained motoneurons..... | 19 |
| 3 Results..... | 20 |
| 3.1 Location of MR and IR MIF motoneuron in case MUS | 20 |
| 3.2 Distribution of the dendrites of MR and IR MIF motoneurons | 28 |
| 3.2.1 Distribution of the dendrites of C-group motoneurons in case MUS | 28 |
| 3.2.2 Distribution of the dendrites of IR MIF motoneurons in case B55..... | 36 |
| 3.2.3 Comparison of MR and IR MIF motoneurons | 41 |
| 4 Discussion | 42 |
| 4.1 Location of MIF motoneurons in the oculomotor nucleus..... | 42 |
| 4.2 Tracer properties | 44 |
| 4.3 The function of C-group motoneurons in vergence eye movements | 46 |
| 4.4 Relationship of C-group motoneurons with Edinger-Westphal nucleus..... | 47 |
| 5 Conclusions | 51 |
| 6 Literature cited | 52 |

| | | |
|---|------------------------|----|
| 7 | Attachment | 63 |
| 8 | Acknowledgements | 65 |
| 9 | Curriculum Vitae..... | 66 |

Abstract

The extraocular muscles in mammals, the effector organs of the oculomotor system, are fundamentally different from skeletal muscle. All extraocular muscles consist of two different layers, an orbital and a global layer. There are two basic categories of the muscle fibers: twitch or singly-innervated muscle fiber (SIF) and non-twitch or multiply-innervated muscle fiber (MIF). Previous studies in monkey revealed that SIF and MIF motoneurons are anatomically separated and have different premotor inputs. SIF and MIF motoneurons were identified by tracer injection into the belly, or the distal myotendinous junction, of the eye muscles. There are two groups of MIF motoneurons in the oculomotor nucleus, the C- and S-group. The C-group motoneurons innervate the medial rectus (MR) and inferior rectus (IR), while S-group motoneurons innervate the superior rectus and inferior oblique muscles. The motoneurons of C-group are located around the periphery of the oculomotor nucleus. We investigated the location of MR and IR MIF motoneurons in C-group, and the dendritic spread of MR compared with IR MIF motoneurons. We found that the MR and IR MIF motoneurons are two different populations of neurons in C-group. They lie relatively separated. The MR MIF motoneurons are located more dorsomedially than IR MIF motoneurons. The pattern of dendritic spread of these two MIF motoneurons is also different. The dendrites of IR MIF motoneurons spread into the supraoculomotor area bilaterally, but do not approach the Edinger-Westphal nucleus, in contrast, the dendrites of MR MIF motoneurons extend into the supraoculomotor area and the Edinger-Westphal nucleus unilaterally. The function of Edinger-Westphal nucleus is associated with the “near response”. In conclusion, the different location and different dendritic trees suggest that MR and IR MIF motoneurons have different functions. The IR MIF motoneurons may help to stabilize the eye position along with MIF motoneurons from other eye muscles, while the MR MIF motoneurons might also participate the vergence eye movements.

Zusammenfassung

Die Augenmuskeln der Säugetiere unterscheiden sich grundsätzlich von der Skelettmuskulatur. Sie bestehen aus zwei unterschiedlichen Schichten, der globalen und der orbitalen Schicht. Diese setzen sich aus zwei Hauptklassen von Muskelfasern zusammen: den einfach innervierten Fasern (SIF) und den multipel innervierten Fasern (MIF). Vorausgegangene Studien an Affen zeigten, dass SIF- und MIF-Motoneurone anatomisch getrennt liegen und unterschiedliche prämotorische Eingänge erhalten. SIF und MIF Motoneurone der Augenmuskeln konnten durch Tracer-Injektionen in den Muskelbauch oder den distalen Muskel-Sehnen-Übergang identifiziert werden. Im Nucleus oculomotorius existieren zwei Gruppen von MIF Motoneuronen, C- und S-Gruppe genannt. Motoneurone der C-Gruppe innervieren den Medialis Rectus (MR), sowie den Inferior Rectus (IR), während die Motoneurone der S-Gruppe den Superior Rectus und den Inferior obliquus Muskel innervieren. C-Gruppen Motoneurone sind in der Peripherie des Nucleus oculomotorius anzufinden.

Unser Ziel war es herauszufinden, wie die MIF Motoneurone des MR und IR innerhalb der C-Gruppe angeordnet sind und wohin deren Dendriten verlaufen. Unsere Ergebnisse zeigen, dass MR und IR MIF-Motoneurone zwei unterschiedliche Neuronenpopulationen in der C-Gruppe bilden und zudem relativ getrennt voneinander angesiedelt sind. Die MIF-Motoneurone des MR liegen weiter dorso-medial als die des IR. Auch die Verbreitungsmuster der Dendriten beider MIF-Motoneurone sind sehr unterschiedlich. Die Dendriten der MIF-Motoneurone des IR ziehen bilateral in das periaquaeduktalen Höhlengrau oberhalb des Nucleus oculomotorius, nicht aber in den Edinger-Westphal Nucleus. Im Gegensatz dazu breiten sich die Dendriten der MR MIF-Motoneurone sowohl in das periaquaeduktale Höhlengrau oberhalb des Nucleus oculomotorius als auch in den Edinger-Westphal Nucleus unilateral aus.

Zusammenfassend lässt sich sagen, dass die unterschiedliche Lokalisation und Ausbreitung der Dendriten eine divergierende Funktion der MIF Motoneurone von MR und IR vermuten lässt. Unsere jetzige Hypothese ist, dass die MIF-Motoneurone des Inferior Rectus helfen, in Zusammenarbeit mit den MIF Motoneuronen der anderen Augenmuskeln, die Position der Augen zu stabilisieren, während die MIF-Motoneurone des MR an den Vergenzbewegungen des Auges beteiligt sind.

Abbreviations

| | |
|--------|--|
| AM | anteromedian nucleus |
| AChR | acetylcholine receptor |
| ChAT | choline acetyltransferase |
| COX | cytochrome oxidase |
| CSPG | chondroitin sulphate proteoglycans |
| CTB | cholera toxin subunit B |
| DAB | diaminobenzidine |
| EOM | extraocular muscles |
| EW | Edinger-Westphal nucleus |
| IO | inferior oblique muscle |
| IP | posterior interposed nucleus |
| IR | inferior rectus muscle |
| LP | levator palpebrae superioris |
| LR | lateral rectus muscle |
| Lvc | lateral visceral cell column |
| MIF | multiply innervated fiber |
| MLF | medial longitudinal fasciculus |
| MR | medial rectus muscle |
| MRF | mesencephalic reticular formation |
| MVNmag | medial vestibular nucleus pars magnocellular |
| MVNp | medial vestibular nucleus pars parvocellular |
| NIII | oculomotor nucleus |
| NIV | trochlear nucleus |
| NVI | abducens nucleus |
| NP-NF | non-phosphorylated neurofilament |
| PBS | phosphate buffer solution |
| PPH | nucleus prepositus hypoglossi |
| PPRF | paramedian pontine reticular formation |
| PON | pretectal olivary nucleus |
| PV | parvalbumin |
| SIF | singly innervated fiber |
| SO | superior oblique muscle |
| SOA | supraoculomotor area |

| | |
|---------|--|
| SR | superior rectus muscle |
| TMB | tetramethylbenzidine |
| VTA | ventral tegmental area |
| VOR | vestibulo-ocular reflex |
| WGA-HRP | wheat germ agglutinin conjugated to horseradish peroxidase |

1 Introduction

1.1 Extraocular muscles

The extraocular muscles (EOM) are the effector organs for voluntary and reflexive movement of the eyes. The presence of six extraocular muscles, four recti (superior, inferior, medial and lateral recti muscles) and two obliques (superior and inferior oblique muscles) is constant among all vertebrate classes, with only a minor variation in arrangement and innervation (Isomura, 1981) (Fig. 1). The four recti and the superior oblique muscle have their origin at the annulus of Zinn, a tendinous ring which surrounds the optic foramen, a portion of the superior orbital fissure, and envelops the optic nerve (Sevel, 1986). In contrast, the inferior oblique muscle arises from the maxillary bone in the medial wall of the orbit. The superior oblique muscle differs from all other extraocular muscles by passing through the trochlea, a tendinous ring attached to the medial orbit, before reaching the globe. Another extraocular muscles called levator palpebrae superioris (LP), which elevates the upper eyelid, is present only in mammals. The levator palpebrae superioris is not attached to the globe, but reaches into the upper lid. In addition to the principal extraocular muscles, many vertebrates possess accessory EOMs, such as the retractor bulbi muscles. The retractor bulbi muscles are correlated with the presence of a nictitating membrane and both structures act synergistically in reflex retraction of the globe in response to the corneal stimulation. However these muscles are not well developed in primates. Up to now, electrophysiological studies have supported the theory that all extraocular muscles participate in all types of eye movements such as vergence, saccades, smooth pursuit, gaze-holding, vestibulo-ocular reflex (VOR), and the optokinetic reflex (Robinson, 1970; Mays and Porter, 1984) with the exception of the levator palpebrae superioris and the retractor bulbi muscle. In this study, we consider only the six extraocular muscles.

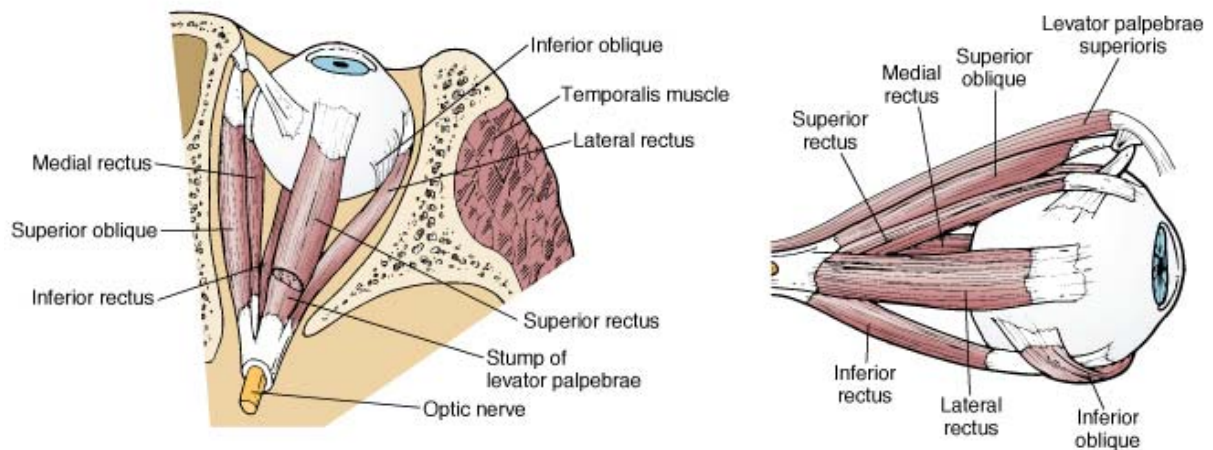


Fig. 1 Schematic drawing of a right human eyeball viewed from dorsally and laterally (Adapted from Lippincott Williams & Wilkins, Pathophysiology: Concept of Altered Health states, Seventh Edition, 2005).

1.1.1 Structure of extraocular muscles

The extraocular eye muscles are unique striated muscles that differ in many respects from skeletal muscles. They consist of an outer orbital layer adjacent to the orbital bone, and an inner global layer adjacent to the eye globe. Sheep possess a distinct third muscle layer (Harker, 1972) which lies mainly distally in a C-shape around the outside of the orbital layer, the peripheral patch layer. There are also reports that a third layer outside the orbital layer in humans, called the marginal layer (Wasicky et al., 2000). In the recti muscles, the orbital layer is comprised of smaller diameter fibers and typically is C-shaped, encompassing the global layer except for a gap left adjacent to the optic nerve or globe. In the oblique muscles, the orbital layer often completely encircles the global layer. The global layer extends over the full muscle length from its origin at the annulus of Zinn to a well-defined tendon at the limbus of the globe (for review see: Porter et al., 1995; Spencer and Porter, 2006). In contrast the orbital layer ends before the muscle becomes tendinous (Oh et al., 2001), and is thought to insert on collagenous pulleys, around the equator of the eyeball, anatomically referred to as the Tenon's capsule (Demer et al., 2000; Oh et al., 2001; Demer, 2002). In addition to the differences of

the myofibers diameter, the two EOM layers are distinguished by substantial morphologic and immunocytochemical differences. First, the orbital layer has a more developed mitochondrial content, oxidative enzyme activities and microvascular network, which all correlate with high fatigue resistance and continuous activation. Second, the orbital layer expresses traits usually associated with developing skeletal muscle. While traditional skeletal myofibers exhibit a developmental transition in expression of embryonic to neonatal to adult myosin heavy chain isoforms, the adult orbital layer myofibers retain the embryonic myosin heavy chain (Wieczorek et al., 1985; Jacoby et al., 1990). Neural cell adhesion molecule, a cell surface molecule normally downregulated during myogenesis, also persists on virtually all orbital, but only some global layer fibers (McLoon and Wirtschafter, 1996). A similar pattern is apparent for the embryonic acetylcholine receptor (AChR) subunit, which is present at all neuromuscular junctions of orbital layer myofibers, but only at those of some global layer myofibers (Kaminski et al., 1996). The orbital and global layers have differences in gene expression (Khanna et al., 2004). Several slow/cardiac muscle markers are preferentially expressed in the orbital layer. This suggests that the orbital layer may be functionally slower than the global layer (Spencer and Porter, 2006).

1.1.2 Different types of extraocular muscles fibers

There are four basic skeletal muscle fiber types that differ on the basis of their biochemical (Moore and Schachat, 1985), histochemical (Brooke and Kaiser, 1970), immunohistochemical (Pierobon-Bormioli et al., 1981), ultrastructural (Schiaffino et al., 1970) and physiological (Burke, 1981) properties. They are slow twitch, fatigue-resistant; fast twitch, fatigue-resistant; fast twitch, fatiguable; fast twitch, intermediate. The myofibers in mammalian EOM are atypical of the skeletal system. Six fiber types can be distinguished in extraocular muscles. All of these fibers can be divided into two basic categories: the twitch or singly-innervated muscle fiber (SIF) and non-twitch or multiply-innervated muscle fiber (MIF) (review: Mayr et al., 1975; Morgan and Proske 1984; Spencer and Porter, 1988) (Fig. 2). Siebeck and Krüger (1955) originally identified two basic extraocular muscle fiber types which are characterized as “Fibrillenstruktur” and “Felderstruktur” fibers, equivalent to the SIFs and MIFs, respectively. The orbital layer contains two fiber types, one SIF and one MIF. And the global layer contains four fiber types, three SIFs and one MIF.

The twitch muscle fibers, or SIFs, are the type of muscle fibers that constitute all the skeletal muscles. They respond to the electrical stimulation with an “all-or-nothing” reaction

that propagates along the whole length of the fiber. The SIFs are innervated by relatively large nerves (7-11 μ m), which terminate as “en plaque” motor endplates in an endplate zone occupying the central third of the muscle(Büttner-Ennever, 2006).

The non-twitch muscle fibers, or MIFs, occur more widely in reptilian and avian skeletal muscles, but in mammals they are found in the extraocular muscles. These fibers are fatigue resistant and respond to electrical stimulation with a slow tonic contraction, which is not propagated along the muscle fiber (Bondi and Chirandini, 1983). They are innervated by a myelinated nerve fiber, which is usually of small caliber (3-5 μ m), so the motor endplates are typically small and distributed all along the length of the fiber, but have a higher density in the distal half of the muscle. At the distal tip of the eye muscle, as it inserts into the tendon, the global layer MIFs are capped by a tangle of nerve terminals called palisade endings, or myotendinous cylinders (Dogiel, 1906; cat: Alvarado-Mallart and Pincon Taymond, 1979; monkey: Ruskell, 1978; human: Richmond et al., 1984; Lukas et al., 2000; Ruskell, 1999.). This characteristic is an exclusive property of the MIFs in the global layer, not possessed by the orbital MIFs or the SIFs.

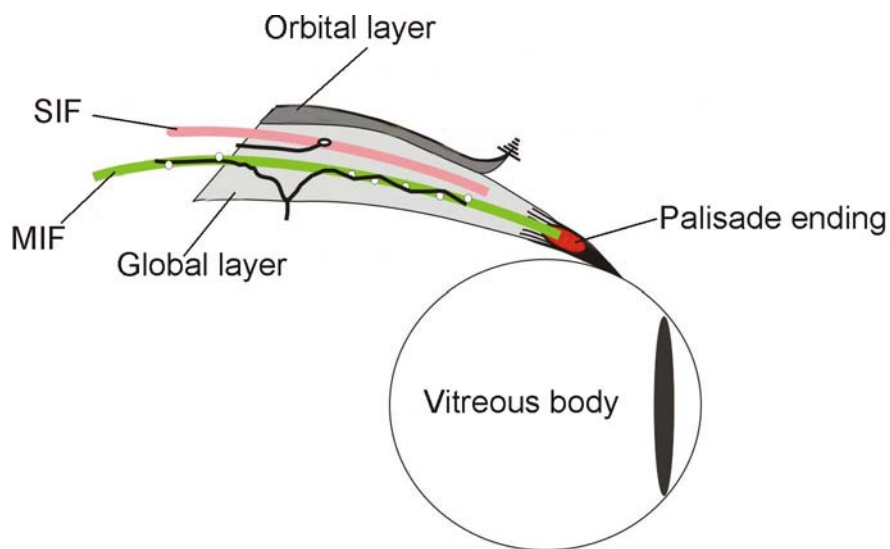


Fig. 2 Schematic drawing of orbital and global layers of monkey eye globe. The Singly innervated fiber (SIF) and multiply innervated fiber (MIF) are two basic fiber types in the extraocular muscles. At the distal tip of the eye muscles, multiply innervated fibers capped by palisade endings appear only in the global layer.

1.2 Motoneurons of extraocular muscles

The basic anatomical organization of the three extraocular motor nuclei controlling the six principal extraocular muscles shows a very constant pattern across various vertebrate classes (review, Büttner-Ennever, 2006). Motoneurons of the oculomotor nucleus (NIII) innervate the ipsilateral medial rectus (MR) and inferior rectus (IR), inferior oblique (IO) and contralateral superior rectus (SR) muscles. Motoneurons of the trochlear nucleus (NIV) control the contralateral superior oblique muscle (SO). The abducens nucleus (NVI) motoneurons drive the lateral rectus (LR) muscle. In addition to the motoneurons of LR, the NVI contains several other neuronal populations, such as abducens internuclear neurons, floccular-projecting neurons. The abducens internuclear neurons that project to the contralateral NIII providing the anatomical basis for conjugate horizontal eye movements (Büttner-Ennever and Akert, 1981; Büttner-Ennever, 2006). The subgroups of motoneuron in NIII are organized in the sequence of IR, MR, IO, SR (and LP) from rostral to caudal (Shaw and Alley, 1981) (Fig. 3). Büttner-Ennever et al., (2001) identified the location of non-twitch motoneurons that innervate the MIFs in the extraocular muscles of the macaque monkey by retrograde labelling. Two anatomically separated sets of SIF and MIF motoneurons are located by tracer injection into the belly or the distal myotendinous junction of EOM. Injection in the belly traced all the MIF and SIF motoneurons. While injection in the distal tip of extraocular muscles only traced MIF motoneurons, which innervate the global layer by multiple 'en grappe' endings throughout their extent (Pachter, 1983; Pachter and Colbjornsen, 1983). The orbital MIFs do not insert into the distal tendon. Therefore these experiments predominantly labelled motoneurons of the global MIFs, which are assumed to be mainly global MIF motoneurons.

The SIF motoneurons are found only within the classical oculomotor nuclei. The MIF motoneurons are located around the periphery of the abducens, trochlear and oculomotor nucleus by the injection of retrograde tracers into the distal tips of the eye muscles, avoiding the central endplate zone (Fig. 3). In NIII, the MIF motoneurons of both IR and MR are grouped together mainly on the dorsomedial border and form the C-group (Büttner-Ennever and Akert, 1981; Büttner-Ennever et al., 2001; Spencer and Porter, 1981). In contrast, the MIF motoneurons of the SR and IO are predominantly located bilaterally around the midline, forming the S-group (Wasicky et al., 2004) (Fig. 3). The motoneurons of C-group can be identified in several species such as cat and lesser Galago (Clarke et al., 1987; Sun and May, 1993; Shall et al., 2003). The C-group is clearly separate from the SIF motoneurons of the

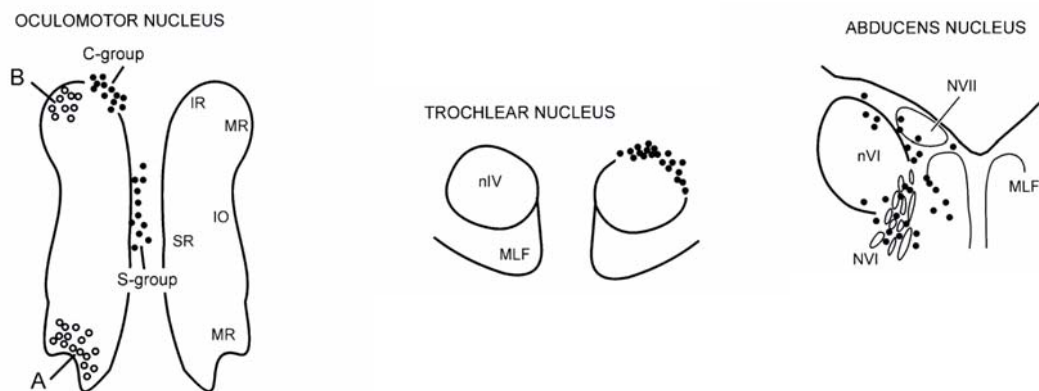


Fig. 3 The MIF motoneurons which innervate mainly the global layer of EOM (black dot), lie around the periphery of NIII, NIV and NVI in a different pattern from the SIF motoneurons. The C-group contains MIF motoneurons from MR and IR; the S-group contains IO and SR MIF motoneurons. The ventral A-group and dorsal B-group contain the MR SIF motoneurons (open circles) in NIII. (Adapted from Büttner-Ennever, *Progress in Brain Research*, 2006)

oculomotor nucleus and lies close to the Edinger-Westphal nucleus (EW), which contains the preganglionic neurons for pupillary constriction and accommodation (Akert et al., 1980; Burde and Willams, 1989; Ishikawa et al., 1990). But large injection into the belly of the MR labelled both MIF and SIF motoneurons, in the C-group, A- and B-groups within or around the NIII. The A- and B-groups are almost entirely MR SIF motoneurons (Eberhorn et al., 2005). The cell size of C-group MIF motoneurons is on average smaller than the A- and B-groups SIF motoneurons. The MIF motoneurons of the SO lie in a compact cluster in the dorsal cap of the trochlear nucleus. The MIF motoneurons of the LR are arranged more loosely around the periphery of the abducens nucleus (Fig. 3), whereas the SIF motoneurons are scattered within the nucleus. The motoneurons of SIFs and MIFs lie separated from each other in NIII, NIV and NVI and have completely different organization of their subgroups (Büttner-Ennever et al., 2001).

Büttner-Ennever et al., (2001) suggest that all the data supports the idea that MIF and SIF motoneurons have different functions. This is further supported by later studies. A major input to the MIF motoneurons of the C- and S-groups is the pretectum (Büttner-Ennever et al., 1996). Using the rabies virus transsynaptic tracing technique, premotor pathways to the abducens nucleus MIF motoneurons were selectively labelled (Ugolini et al., 2006). The premotor inputs to LR MIF motoneurons have been shown to arise from the supraoculomotor area (SOA) and mesencephalic reticular formation (MRF) adjacent to SOA, as well as the areas related with the neural integrator, nucleus prepositus hypoglossi (PPH) and the medial

vestibular nucleus pars parvocellular (MVNp) (Ugolini et al., 2006). But the MIFs do not receive direct input from the premotor saccadic regions such as the paramedian pontine reticular formation (PPRF).

The differences in connectivity of SIF and MIF motoneurons are paralleled by differences in their histochemical properties in monkey. Both motoneurons of SIFs and MIFs are shown to be cholinergic, but in monkey, the MIF motoneurons in the periphery of the motonuclei do not contain non-phosphorylated neurofilaments (NP-NF; labelling by SMI32) and lack the perineuronal nets. In contrast, SIF motoneurons express all markers at high intensity. So the absence of perineuronal nets and non-phosphorylated neurofilaments is a distinctive criterion to identify MIF and SIF motoneurons in other species, including human (Eberhorn et al., 2005).

1.3 Primary function of extraocular muscles and eye movement

The contributions of the four recti and two oblique eye muscles to eye movements depend on the point of rotation of the eye globe, the bony anatomy of the orbit, and the origin and insertion of each eye muscle. The lateral and medial muscles move the eye only in the horizontal plane. Four muscles (superior rectus, inferior rectus, superior oblique and inferior oblique) control the vertical and torsional motion (Fig. 4). The medial rectus and lateral rectus function relatively simply and act as antagonists: the medial rectus as the principal adductor, the lateral rectus as the principal abductor (Fig. 4). With the eyes in the primary position, the primate vertical recti insert on the globe at angle of 23° laterally to the visual axis, they have more or less secondary roles in adduction for both muscles and intorsion for SR and extorsion for the IR. The principal action of superior oblique and inferior oblique muscles is intorsion and extorsion, respectively. For SO and IO, they both have a secondary function: the SO additionally depresses and abducts the globe, the IO elevates and adducts. The primary actions of these six EOMs are similar in the lateral-eyed mammals, though their secondary functions in eye movements differ from those frontal-eyed mammals due to divergent insertion on the globe (Büttner-Ennever, 2006). The need for eye movement is to permit the clear vision of objects, bring the image on small fovea and creating the physiological basis for holding an image steady on the retina. The motoneurons generate motor responses, some with more tonic properties, others with more phasic properties, but all of the motoneurons respond with every type of eye movement (Keller and Robinson, 1972; Fuchs et al., 1985; Dean,

1996). But what is then the function of different types of MIF and SIF motoneurons? It was found that SIF and MIF motoneurons in NIII receive different afferent projections (Wasicky et al., 2004). The inputs to the MIF motoneurons arise from structures involved in more tonic functions, such as gaze-holding (parvocellular parts of medial vestibular nucleus) and areas associated with vergence or object fixation (pretectum). In contrast, the afferents to the SIF motoneurons arise from the area which is related to saccades (PPRF) or the vestibulo-ocular reflex (medial vestibular nucleus pars magnocellular, MVNmag)(Büttner-Ennever et al., 1996; Ugolini et al., 2006).

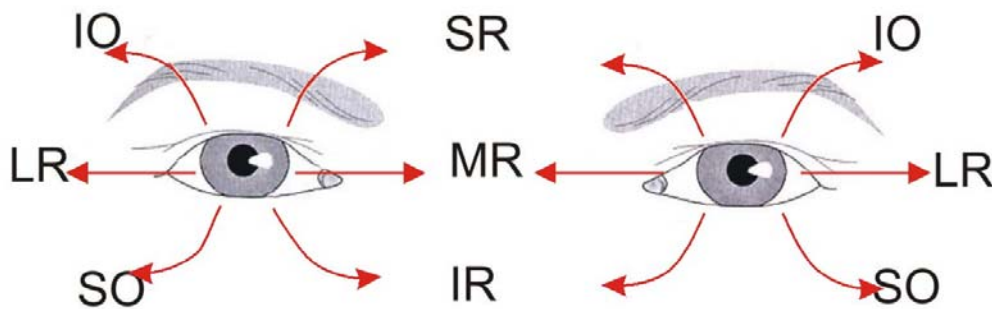


Fig. 4 The rotations of the six extraocular muscles with the eye in the primary position. The lateral and medial rectus muscles move the eye only in the horizontal plane. The rest four extraocular muscles control the eye in the vertical plane. (Adpated from Schünke M et al., 2006. Prometheus Lernatlas der Anatomie. P135)

1.4 Aim

Given that SIF and MIF motoneurons may have different functions, the following questions arise:

1. Are the IR and MR MIF motoneurons two different populations in the C-group, or do they project to both recti?
2. Are the IR and MR MIF motoneurons intermingled or topographically organized in the C-group?
3. What is the overall extent of IR and MR MIF motoneurons dendrites? Do they have the same morphological organization?

In an attempt to answer these questions and understand the function of the C-group better, we labelled IR and MR MIF motoneurons simultaneously to check the location and their other properties.

2 Material and Methods

All experimental procedures conformed with the state and university regulations on Laboratory Animal Care, including the Principles of Laboratory Animal Care (NIH publication 85-23, Revised 1985), and were approved by the Animal Care Officer and Institutional Animal Care and Use Committee.

2.1 Introduction of tract-tracing methods

The purpose of neuronal tracing is to find out the anatomical connections within the nervous system. Tracers are used to ascertain the afferent and efferent of neurons in central nervous system by retrograde and anterograde axonal transport (Fig. 5). Retrograde axonal transport allows identification of the afferent nerve fibers to a particular target zone, while anterograde axonal transport enables the efferent of individual or groups of neurons to be charted within the central nervous system. So for retrograde transport, the tracer is applied to a fiber tract or a terminal target field of innervation, while the anterograde transport, the uptake area is neuron soma and/or its dendrites. Anterograde transport is used in the translocation of membranous organelles (e.g., mitochondria) and vesicles as well as of macromolecules, such as actin, myosin and some of the enzymes necessary for neurotransmitter synthesis at the axon terminals mediated by kinesin-family proteins. Anterograde axonal transport has been shown to have a major fast and a slow component. The slow component is divided into “slow component a” and “slow component b” at rates of approximately 0.1 and 6 mm/day respectively. But these slow components are not involved in the fast component for tracer studies. The protein building blocks of neurofilaments, subunits of microtubules, materials taken up by exocytosis (e. g., viruses and toxins) returned to the cell body from the axon by retrograde transport mediated by dyneins (Fig. 6). The fast component of transport demonstrates distinct maximal rates for anterograde (200-400 mm/day) and retrograde (100-200mm/day) transport. In this study, the tracer wheat germ agglutinin conjugated to horseradish peroxidase (WGA-HRP) and cholera toxin subunit B (CTB) were injected into the eye muscles and retrogradely transported to the appropriate region of brain. But the tracer WGA-HRP and CTB have different sensitivity and staining method for the tract tracing. The labelled cells and terminals can be made visible by light microscopy technique, after histochemical processing.

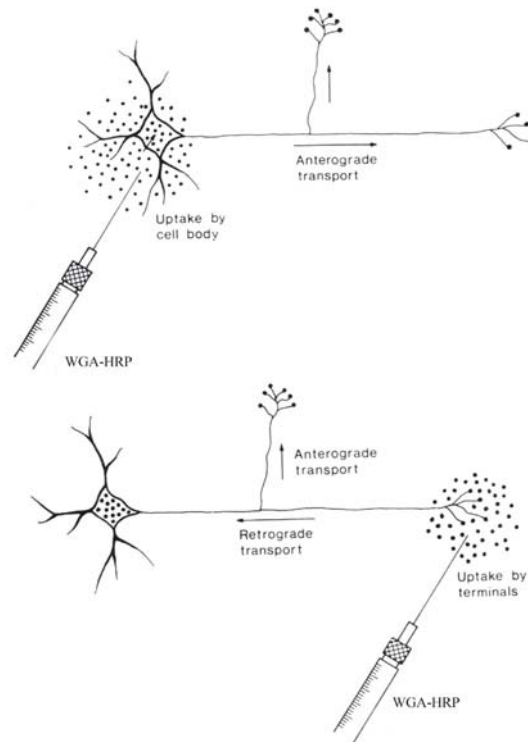


Fig. 5 Schematic drawing of anterograde and retrograde tract-tracing methods of wheat germ agglutinin conjugated to horseradish peroxidase.

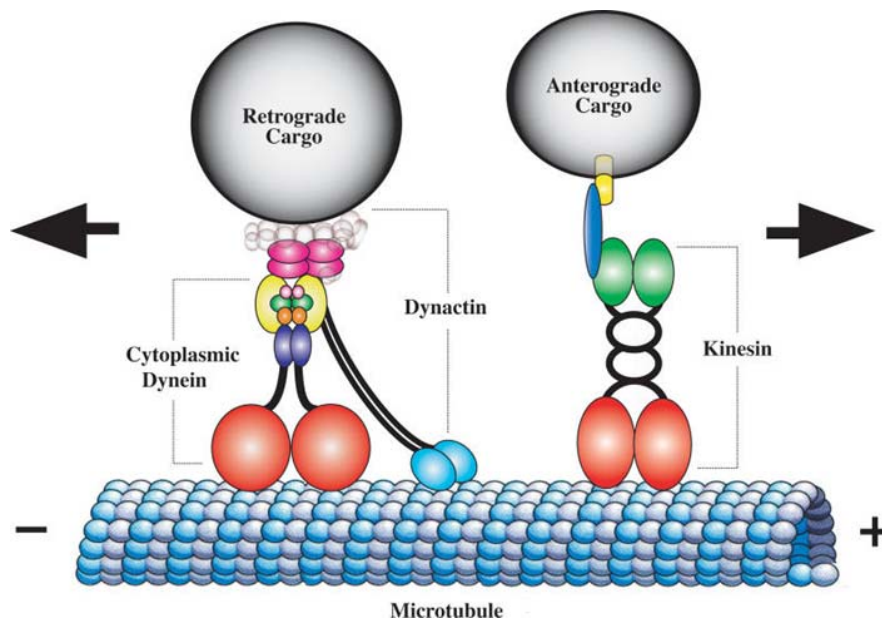


Fig. 6 Schematic diagrams of the microtubule motor proteins cytoplasmic dynein and kinesin. Cytoplasmic dynein transports cargo in the retrograde direction toward the minus ends of microtubules whereas kinesin transports cargo in the anterograde direction toward the plus ends. (Adapted from Duncan JE and Goldstein LS. 2006. The genetics of axonal transport and axonal transport disorders. PLoS Genet. 2: e124.)

2.1.1 Tracer WGA-HRP

Horseradish peroxidase (HRP) is based on the retrograde transport of material from axon terminals to cell body. In the current tract-tracing studies, the lectin wheat germ agglutinin conjugated to the enzyme HRP was used. Lectins are naturally occurring proteins or glycoproteins that bind to cell membranes and stimulate micropinocytosis. The presence of WGA molecules greatly enhances HRP uptake by neurons, so that WGA-HRP is taken up by both cell body and axon terminal at the site of injection. This compound is widely used as both anterograde and retrograde tracer.

2.1.2 Tracer cholera toxin subunit B

Cholera toxin subunit B (cholera toxin B subunit, CTB), the non-toxic component of cholera toxin, binds to GM1 gangliosides on neuronal cell surfaces. As a consequence of this phenomenon, cholera toxin B subunit undergoes internalization followed by retrograde axonal transport. Unlabelled, this neuronal cell marker can be visualized using antibodies and classical immunocytochemical techniques. Its detection can be combined with other immunocytochemical procedures, for instance that for neurotransmitter identification or neuropeptide detection. Irrespective of which detection system is employed, this tracer has proven to be a reliable marker in tracing strategies both in peripheral nervous structures and in central nervous systems.

2.2 Injection of tracer

Macaque monkeys were anesthetized with sodium pentobarbital 30mg/kg. Under sterile conditions, the extraocular muscles were exposed by retracting the eyelid, making a conjunctival incision, and partially collapsing the eyeball. The neuron tracers cholera toxin subunit B (5 μ l, 1%, from List Biological Laboratories, 703) and Wheat germ agglutinin conjugated to horseradish peroxidase (WGA-HRP, 5 μ l, 2.5%, Sigma) were injected through a Hamilton syringe into the distal tip of the eye muscles (Fig. 7). In case MUS, CTB was injected into the distal tip of right MR, while WGA-HRP was injected into the distal tip of right IR. In case B55, CTB was only injected into the distal tip of IR (Table 1).

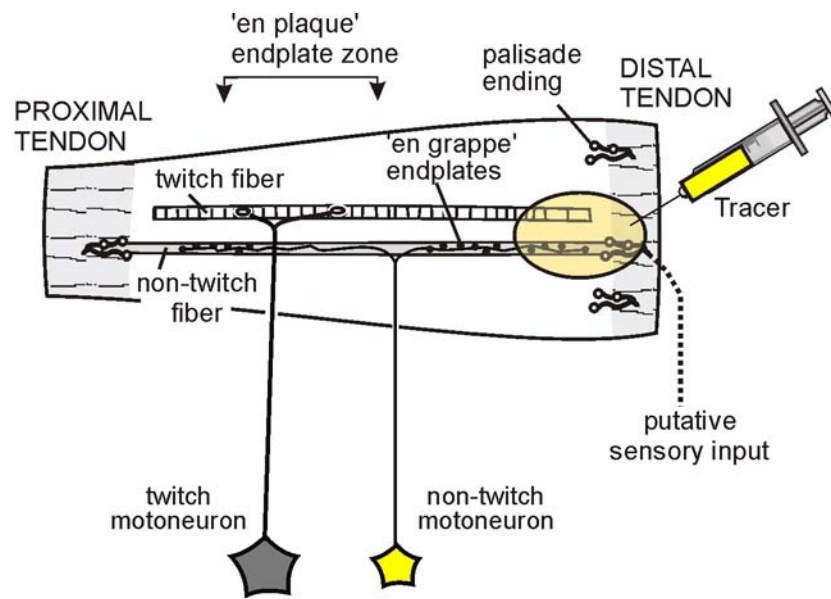


Fig. 7 The structure of an eye muscle, shows that the SIF with a central "en plaque" endplate zone, and MIF with "en grappe" terminals along the whole muscle. The tracer is injected into the distal tip of tendon, so only MIF motoneurons of the global layer will be labelled.

| Case \ Muscle | MR | IR |
|---------------|--------|--------------|
| MUS | 1% CTB | 2.5% WGA-HRP |
| B55 | ----- | 1% CTB |

Table 1. Two cases with different tracer injection. The tracers were injected into the distal tip of the right eye muscles.

2.3 Perfusion

After a survival time of 3 days, the animals were killed with an overdose of Nembutal (80 mg/kg body weight) and perfused with 0.9% saline (37° C) to clean all the blood, then followed by 3 liters 4% paraformaldehyde in a 0.1M phosphate buffer solution (PBS; pH 7.4).

The brains were removed from the skull. The brains were immersed in 10% sucrose in 0.1M phosphate buffer (pH 7.4) and transferred to 30% sucrose for 4 days under 4° C. The brains were cut at 40 µm on a freezing microtome in the transverse stereotaxic plane.

2.4 Immunocytochemical labelling

2.4.1 WGA-HRP immunocytochemical labelling

Free-floating brain sections of the WGA-HRP injection case (MUS) were reacted with 0.05% diaminobenzidine (DAB) and Cobalt-Chlorid, which yield a black reaction product in retrogradely labelled motoneurons. These series underwent a second protocol for the detection of tracer CTB.

2.4.2 Cholera toxin subunit B immunocytochemical labelling

After the DAB-Co reaction, the labelled sections were processed for the immunohistochemical reaction of the tracer CTB. After blocking with 5% normal donkey serum in 0,1M PBS pH 7,4 containing 0,3% Triton for 1 hour, sections were incubated with goat anti-CTB (1:20,000) overnight, followed by the second antibody rabbit anti-goat (1:200) for 1 hour in room temperature, then followed by Extravidin-Peroxidase (1:1000) for 1 hour. The CTB was visualized with a DAB-reaction, which yields a brown reaction product in retrogradely labelled motoneurons. The sections were counterstained by Nissl staining (with cresyl violet).

2.5 Photographic software and analysis of stained motoneurons

All slides were examined with a Leica microscope DMRB (Bensheim, Germany).

Images of photographs were digitalized by using the 3-CCD video camera (Hamamatsu C5810; Hamamatsu, Herrsching, Germany) mounted on a Leica DMRB microscope. The images were captured on a computer with Adobe Photoshop 5 software. Sharpness, contrast, and brightness were adjusted to reflect the appearance of the labelling seen through the microscope. The pictures were arranged and labelled with drawing software (CorelDraw 8 and 11). The labelled neurons and dendrites of a series of transverse sections through oculomotor nucleus were plotted on the pictures taken with the 3-CCD video camera and displayed on the computer screen with drawing software (CorelDraw 11).

3 Results

3.1 Location of MR and IR MIF motoneuron in case MUS

Tracer injection with CTB into the distal tip of right MR led to brown labelled MR MIF motoneurons in the C-group. While tracer WGA-HRP injection into the distal tip of right IR led to black labelled IR MIF motoneurons in the C-group. The tracer retrogradely labelled the ipsilateral MIF motoneurons of MR and IR, which lay dorsomedially to the oculomotor nucleus. All the retrogradely labelled neurons were plotted from rostral to caudal level of the oculomotor nucleus (Fig. 8-13). In the plotting figures, the dots represent the cell bodies of labelled IR (red) and MR (blue) MIF motoneurons.

For the first question:

The results showed clearly that there were no double-labelled MR and IR MIF motoneurons in the C-group. This means that no MIF motoneurons in C-group project to both MR and IR (Fig. 8c-13c).

For the second question:

The MR and IR MIF motoneurons did not intermingle together in the rostral two-thirds of NIII (Fig. 14). The MR and IR MIF motoneurons in the C-group lay relatively separated, with the MR cell bodies collecting more dorsomedially (Fig. 8c-13c). Generally, the IR MIF motoneurons lay close to the NIII, in contrast, the MR MIF motoneurons lay outside of IR MIF motoneurons group, close to the midline (Fig. 14). Interesting point is that, in the rostral level of sections, there were more labelled MR MIF motoneurons than IR MIF motoneurons (Fig. 14 A, B, C). A few of these labelled MR MIF motoneurons were very close association with EW and located even more dorsally than EW, close to the periaqueductal gray (Fig. 8; Fig.15a). But in the anteromedian nucleus (AM), there were no labelled neurons.

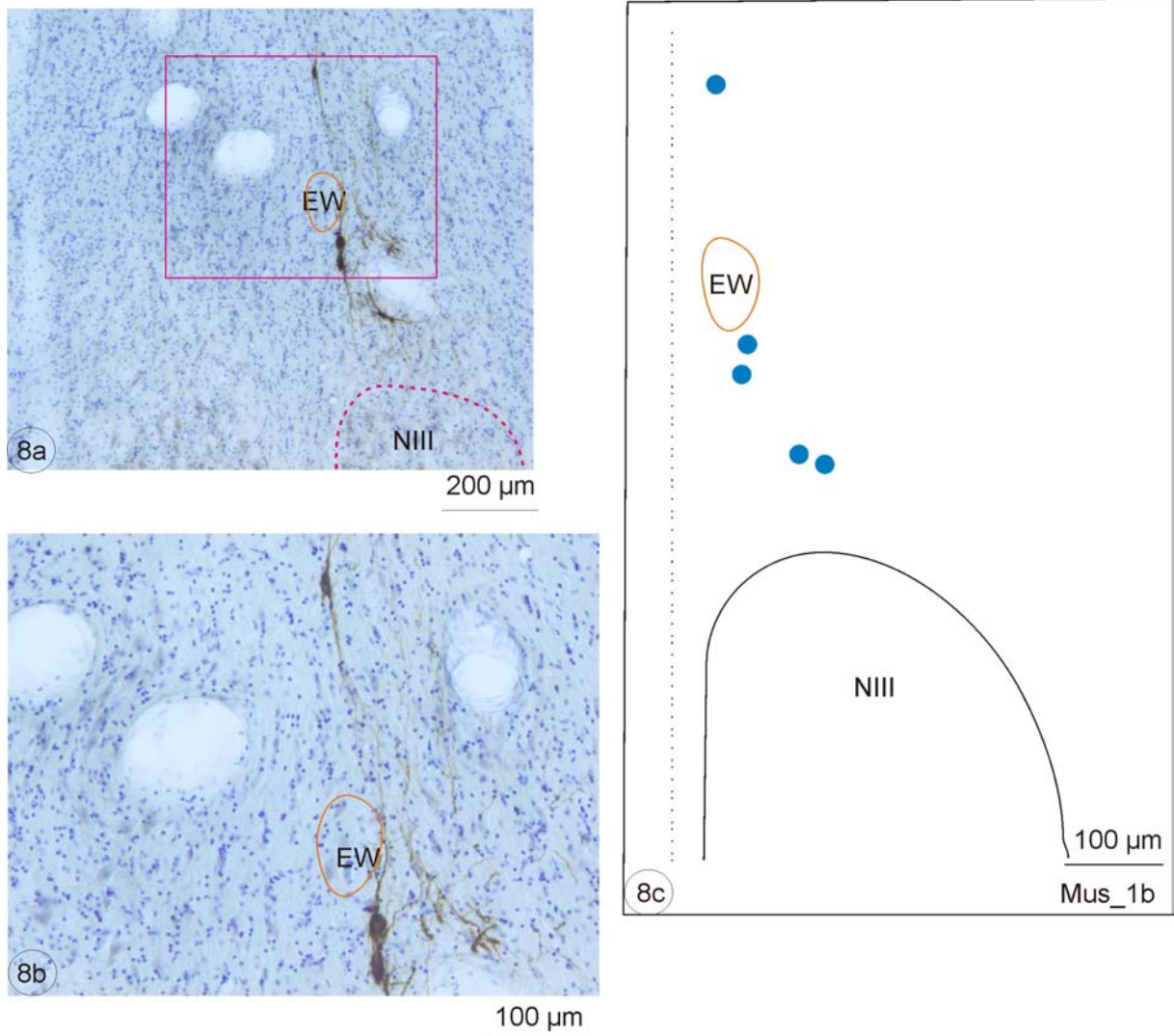


Fig. 8 Photographs and plot of MIF motoneurons of MR and IR labelled by injection the tracer CTB and WGA-HRP into the distal tip of right MR and right IR, respectively. In this section, there was no labelled IR MIF motoneuron. 8a shows the group of labelled MR MIF motoneurons, which lay around the periphery of NIII. Some of these labelled neurons were located even more rostrally than EW. 8b is the detail of the frame in 8a under x10 magnification, showing the labelled neurons. 8c is the plot of the labelled neurons in figure 8a. The blue dots represent the bodies of labelled MR MIF motoneurons.

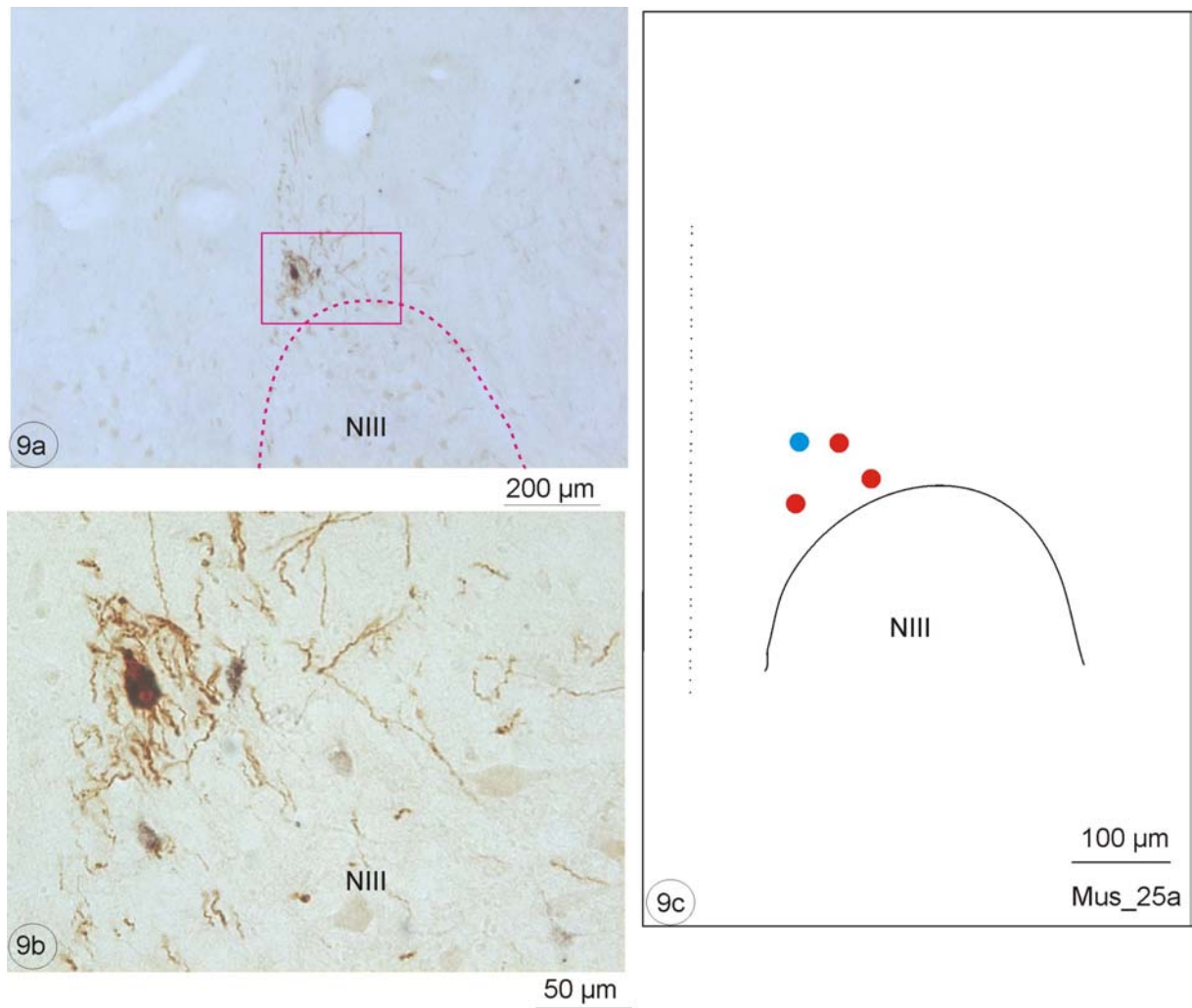


Fig. 9 Photographs and plot of MIF motoneurons of MR and IR labelled by injection the tracer CTB and WGA-HRP into the distal tip of right MR and IR, respectively. 9a shows the group of labelled MR and IR MIF motoneurons, which lay around the periphery of rostral NIII. 9b is the detail of the frame in 9a under x20 magnification, showing the labelled neurons. 9c is the plot of the labelled neurons in figure 9a. The dots represent the bodies of labelled IR (red) and MR (blue) MIF motoneurons.

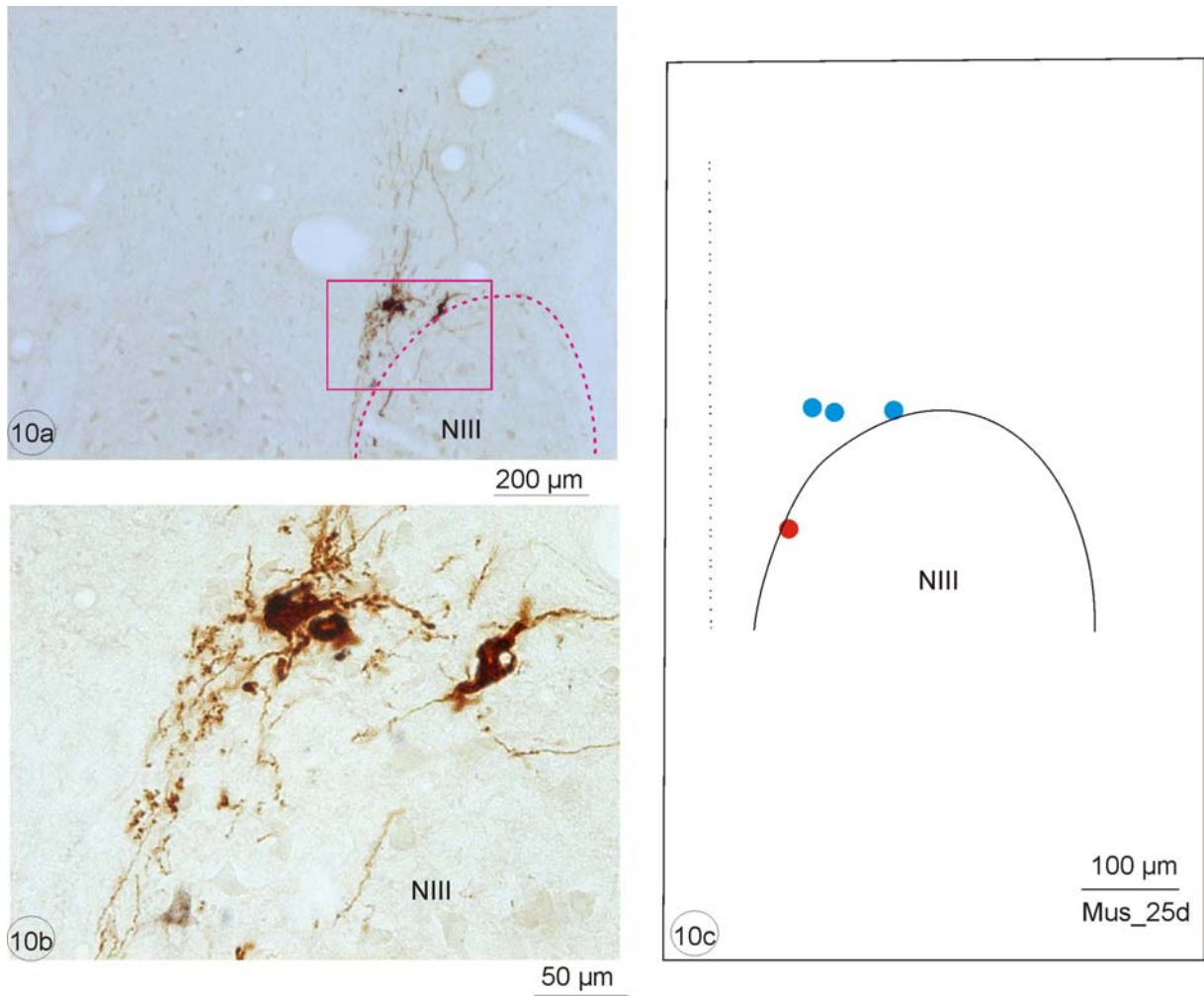


Fig. 10 Photographs and plot of MIF motoneurons of MR and IR labelled by injection the tracer CTB and WGA-HRP into the distal tip of right MR and IR, respectively. 10a shows the group of labelled MR and IR MIF motoneurons, which lay around the periphery of NIII. 10b is the detail of the frame in 10a under x20 magnification, showing the labelled neurons. 10c is the plot of the labelled neurons in figure 10a. The dots represent the bodies of labelled IR (red) and MR (blue) MIF motoneurons.

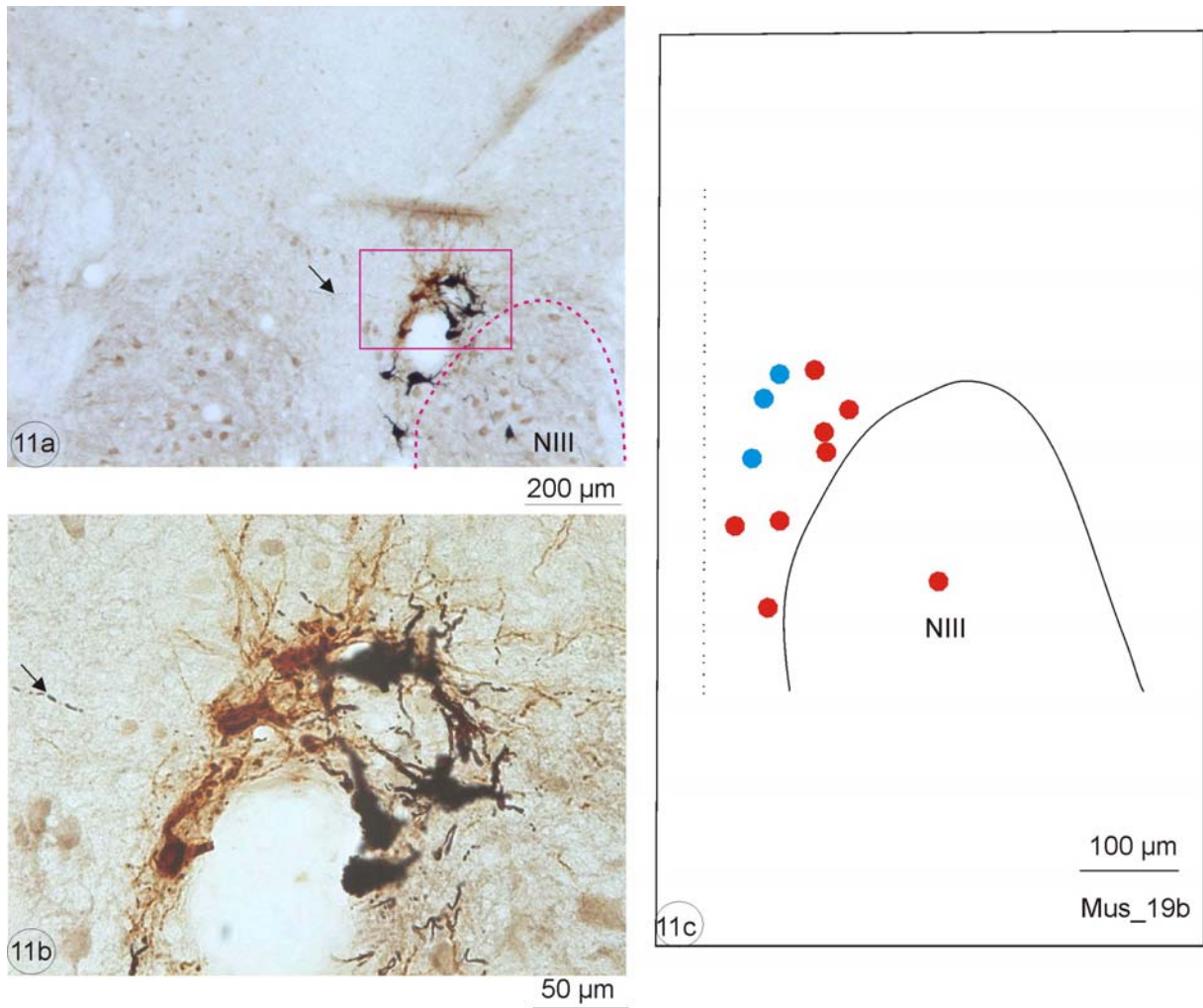


Fig. 11 Photographs and plot of MIF motoneurons of MR and IR labelled by injection the tracer CTB and WGA-HRP into the distal tip of right MR and IR, respectively. 11a shows the group of labelled MR and IR MIF motoneurons, which lay around the periphery of NIII. 11b is the detail of the frame in 11a under x20 magnification, showing the labelled neurons. 11c is the plot of the labelled neurons in figure 11a. The dots represent the bodies of labelled IR (red) and MR (blue) MIF motoneurons. The arrow in 11a, b shows the dendrites of IR MIF motoneurons crossing the midline.

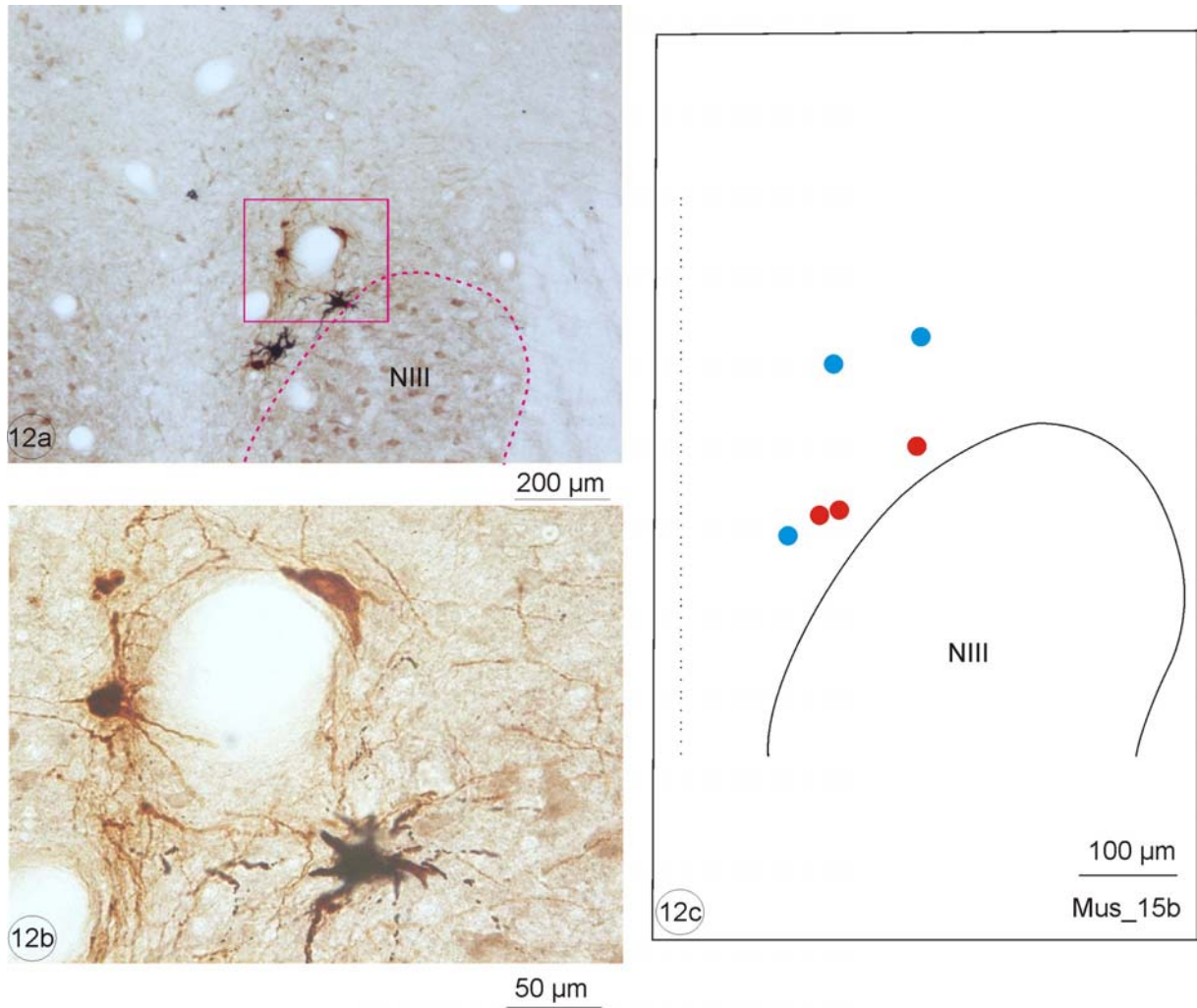


Fig. 12 Photographs and plot of MIF motoneurons of MR and IR labelled by injection the tracer CTB and WGA-HRP into the distal tip of right MR and IR, respectively. 12a shows the group of labelled MR and IR MIF motoneurons, which lay around the periphery of caudal NIII. 12b is the detail of the frame in 12a under x20 magnification, showing the labelled neurons. 12c is the plot of the labelled neurons in figure 12a. The dots represent the bodies of labelled IR (red) and MR (blue) MIF motoneurons.

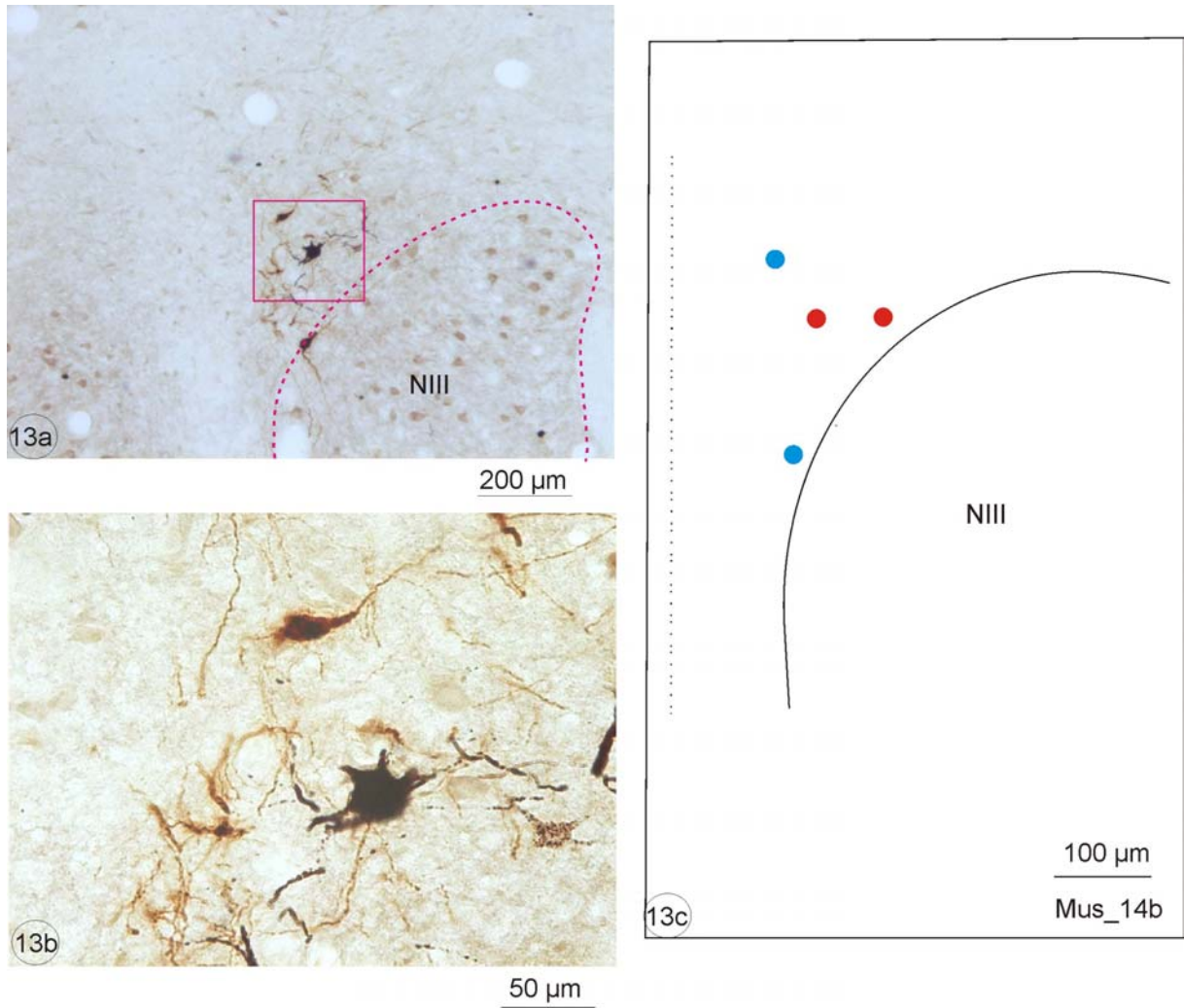


Fig. 13 Photographs and plot of MIF motoneurons of MR and IR labelled by injection the tracer CTB and WGA-HRP into the distal tip of right MR and IR, respectively. 13a shows the group of labelled MR and IR MIF motoneurons, which lay around the periphery of caudal NIII. 13b is the detail of the frame in 13a under x20 magnification, showing the labelled neurons. 13c is the plot of the labelled neurons in figure 13a. The dots represent the bodies of labelled IR (red) and MR (blue) MIF motoneurons.

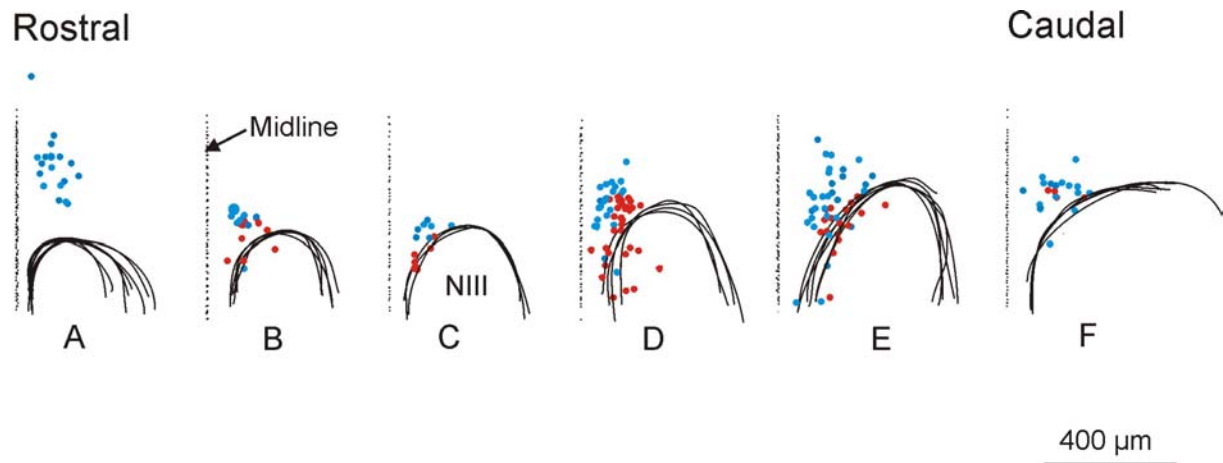


Fig. 14 All the labelled motoneurons were plotted from rostral to caudal level of the oculomotor nucleus by a reference line, midline (the arrow in B). The dots represent the bodies of labelled IR (red) and MR (blue) MIF motoneurons. They both lay around the periphery of the oculomotor nucleus, but the MIF motoneurons of MR were more dorsomedial than IR MIF motoneurons.

3.2 Distribution of the dendrites of MR and IR MIF motoneurons

3.2.1 Distribution of the dendrites of C-group motoneurons in case MUS

Aside from the layered location of IR and MR MIF motoneurons, a different pattern of the dendritic trees was evident. The labelled dendrites were inspected and reconstructed. The black lines represent the dendrites of labelled MR MIF motoneurons. The red lines represent the dendrites of labelled IR MIF motoneurons.

The dendrites of MR MIF motoneurons radiated over the supraoculomotor area and Edinger-Westphal nucleus, but they did not cross the midline, spread only unilaterally and laterally. The dendritic spread was shown in the reconstructed pictures (Fig. 15c, 16c, 17c, 18c, 19c, 20c, 21c). The dendrites of IR MIF motoneurons, which were labelled by the WGA-HRP were not so evident as the dendrites of MR MIF motoneurons that were labelled by CTB in this case MUS. Only the dendritic pattern of MIF motoneurons labelled by CTB was reconstructed. So we reconstructed the dendritic pattern of MR MIF motoneurons in Case MUS and IR MIF motoneurons in Case B55.

But in two sections, dendrites of IR MIF motoneurons clearly spread into the opposite side of injection (Fig. 11a, b; 18a, b, c marked by arrow).

Some labelled neurons inside of the oculomotor nucleus were due to the tracer contamination of the inferior oblique muscle. The SIF and MIF motoneurons of IO were both labelled with the tracer WGA-HRP (arrow head, Fig. 17c-21c). The location of IO SIF and MIF motoneurons is different with the C-group motoneurons. The IO SIF motoneurons are located in the middle part of the oculomotor nucleus, while the IO MIF motoneurons are located in the S-group, which lay around the midline between the oculomotor nuclei. So the labelled IO MIF and SIF motoneurons did not affect the analysis of the C-group motoneurons.

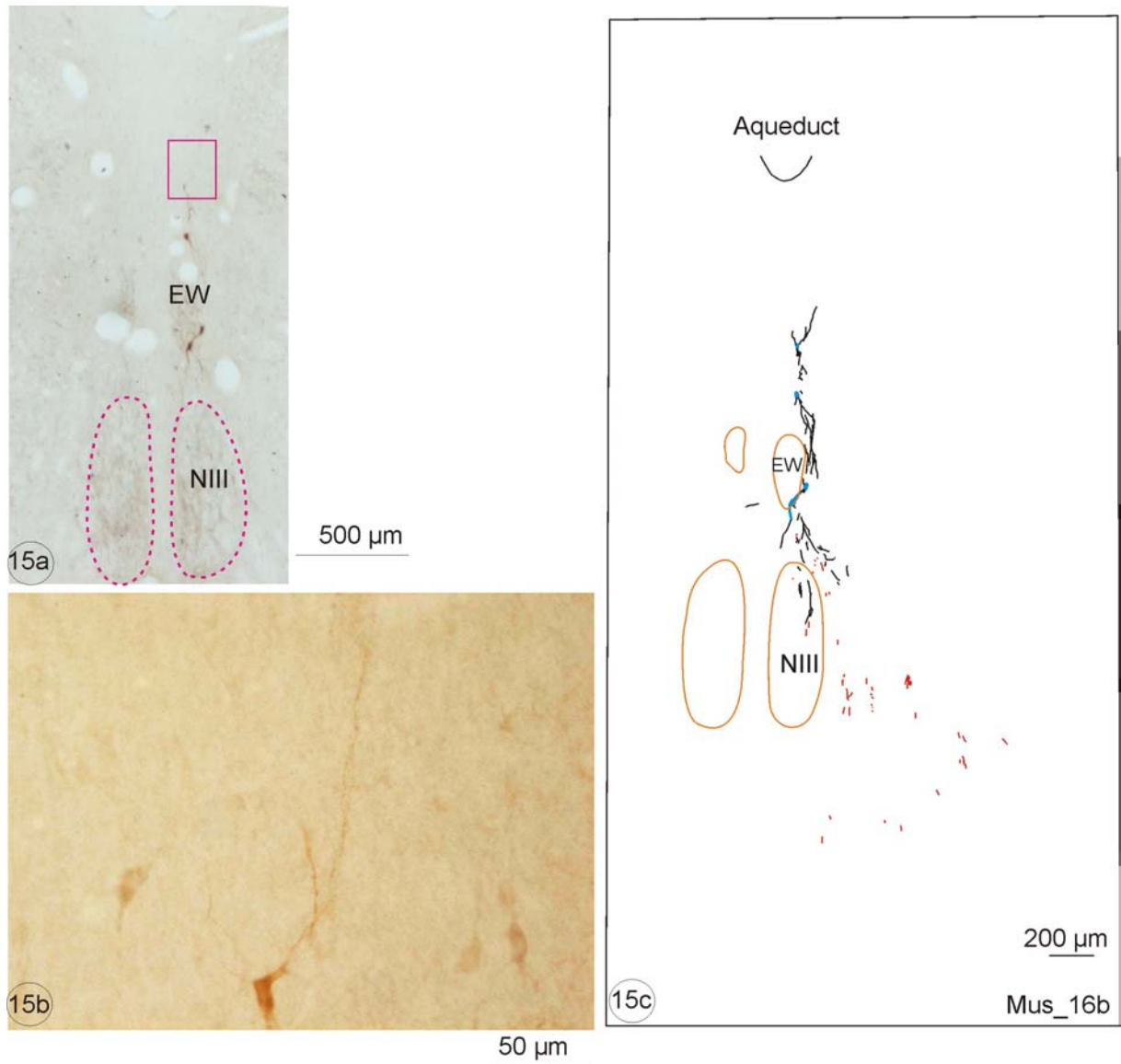


Fig. 15 Photographs and drawings of MIF motoneurons of MR labelled by injection the tracer CTB into the distal tip of right MR. 15a shows the group of labelled MR MIF motoneurons which lie around the periphery of EW. 15b is the detail of the frame in 15a under x20 magnification, showing the labelled dendrites. 15c is the reconstructed figure of labelled neurons and dendrites. The blue parts represent the bodies of the labelled MR MIF motoneurons.

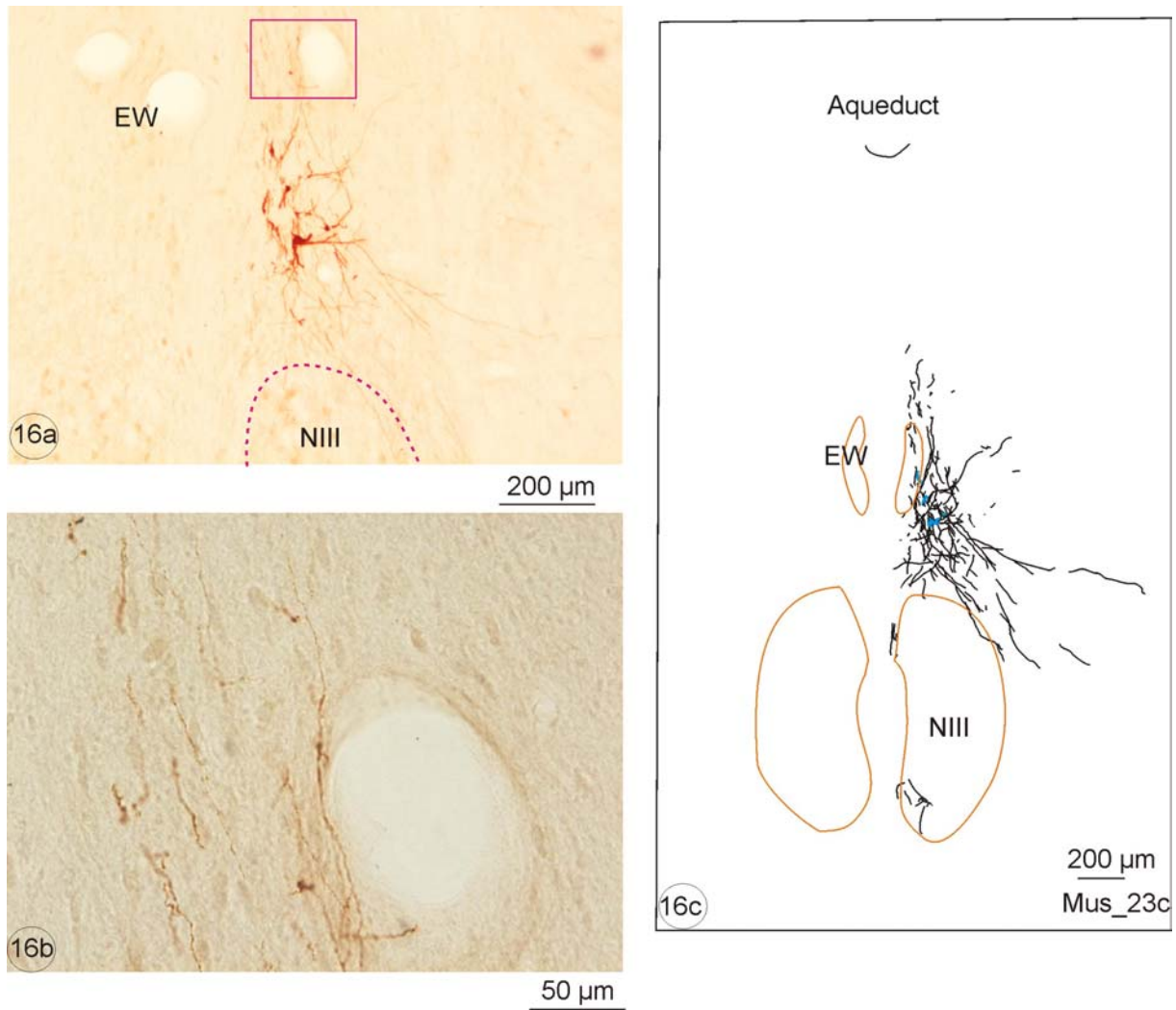


Fig. 16 Photographs and drawings of MIF motoneurons of MR labelled by injection the tracer CTB into the distal tip of right MR. 16a shows the group of labelled MR MIF motoneurons which lie around the periphery of rostral NIII. 16b is the detail of the frame in 16a under x20 magnification, showing the dendrites. 16c is the reconstructed figure of labelled neurons and dendrites. The blue parts represent the bodies of labelled MR MIF motoneurons.

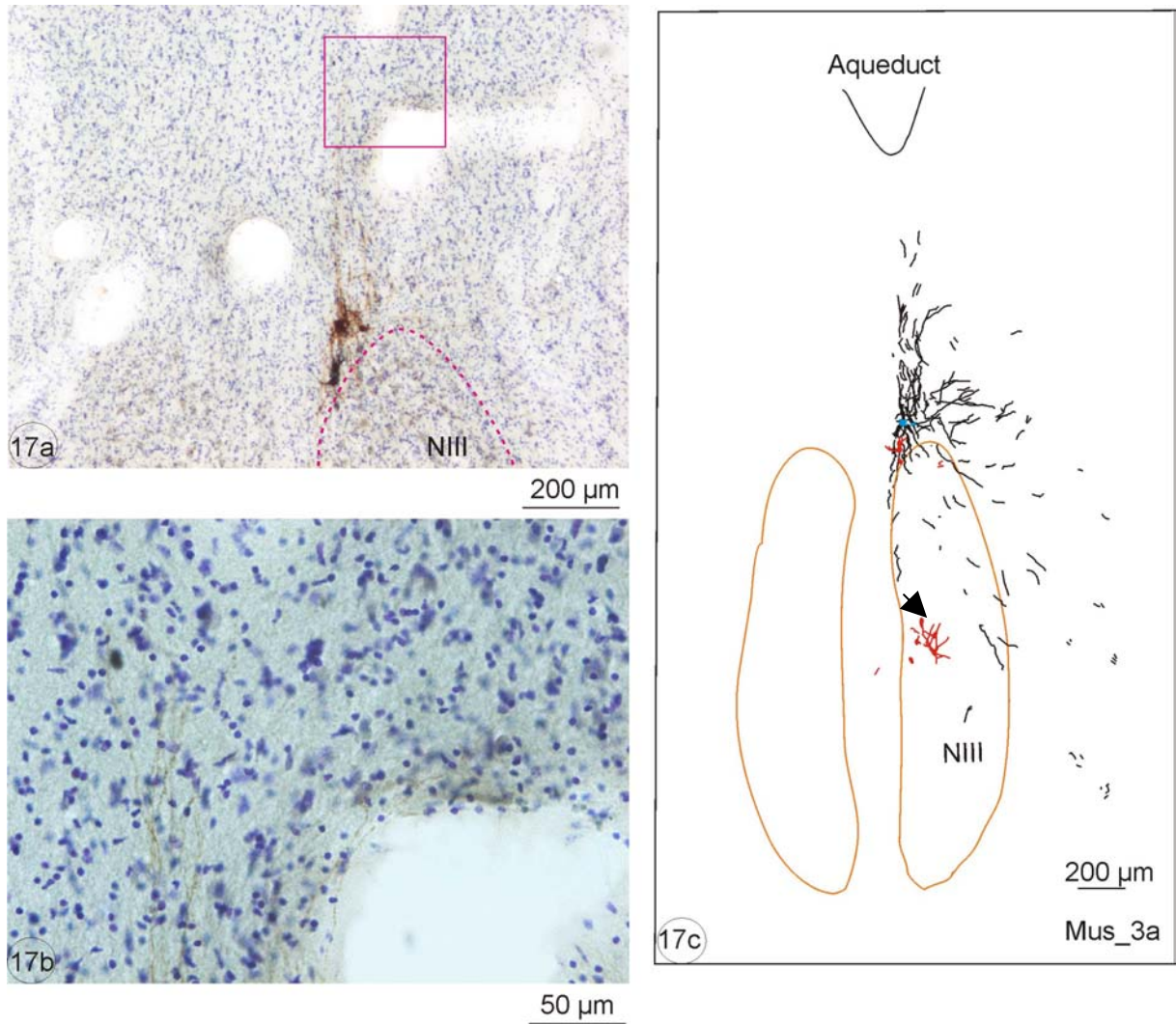


Fig. 17 Photographs and drawings of MIF motoneurons of MR and IR labelled by injection the tracer CTB and WGA-HRP into the distal tip of right MR and IR, respectively. 17a shows the group of labelled MR and IR MIF motoneurons which lie around the periphery of NIII. 17b is the detail of the frame in 17a under $\times 20$ magnification, showing the dendrites. 17c is the reconstructed figure of labelled neurons and dendrites. The red and blue parts represent the bodies of labelled IR and MR MIF motoneurons. The arrow head shows that the labelled neurons were due to the tracer contamination of the IO. The SIF and MIF motoneurons of IO were both labelled with the tracer WGA-HRP.

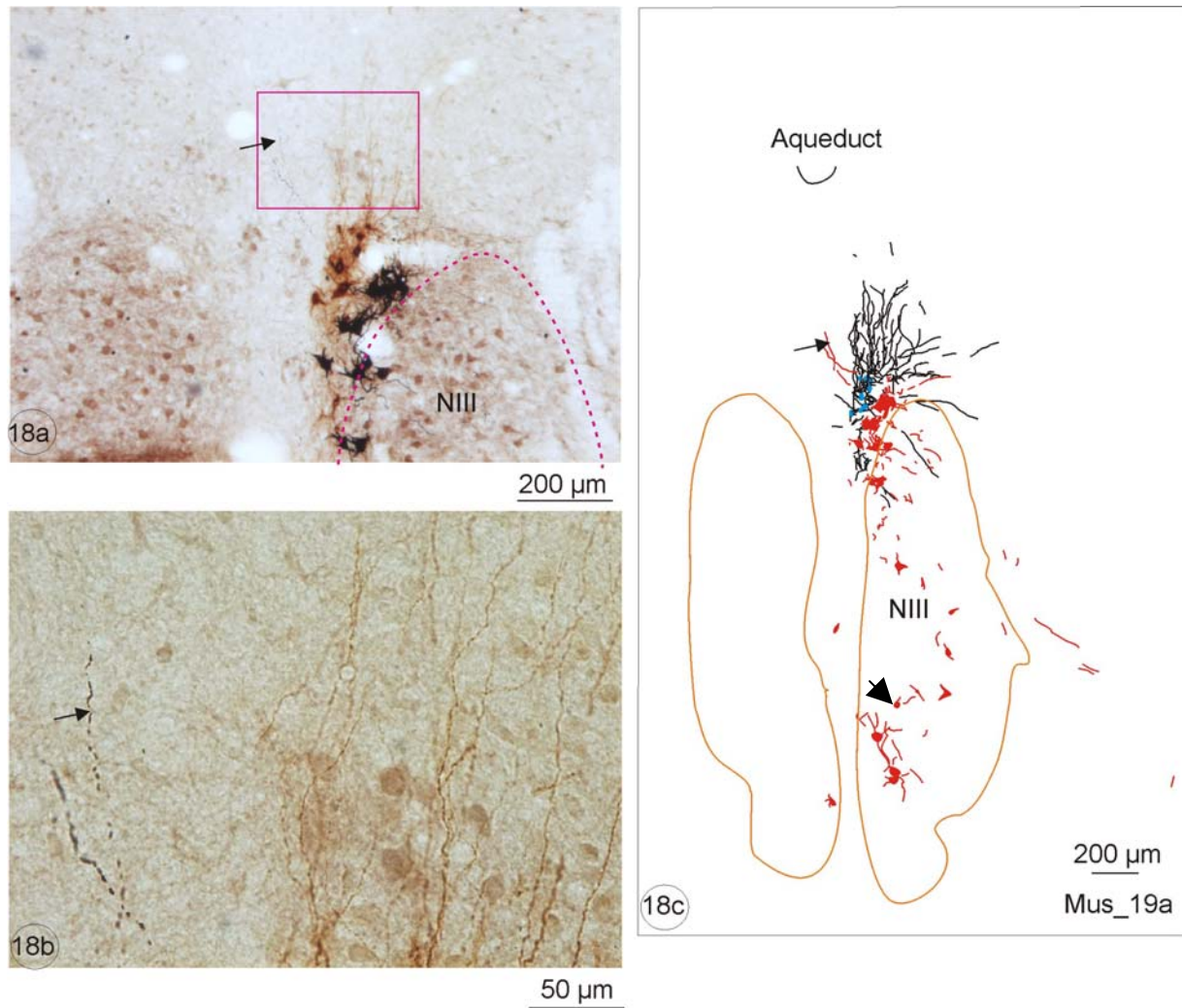


Fig. 18 Photographs and drawings of MIF motoneurons of MR and IR labelled by injection the tracer CTB and WGA-HRP into the distal tip of right MR and IR, respectively. 18a shows the group of labelled MR and IR MIF motoneurons which lie around the periphery of NIII. 18b is the detail of the frame in 18a under x20 magnification, showing the dendrites. 18c is the reconstructed figure of labelled neurons and dendrites. The red and blue parts represent the bodies of labelled IR and MR MIF motoneurons. The arrow shows that the dendrites of IR MIF motoneurons crossed the midline. The arrow head shows that the labelled neurons were due to the tracer contamination of the IO. The SIF and MIF motoneurons of IO were both labelled with the tracer WGA-HRP.

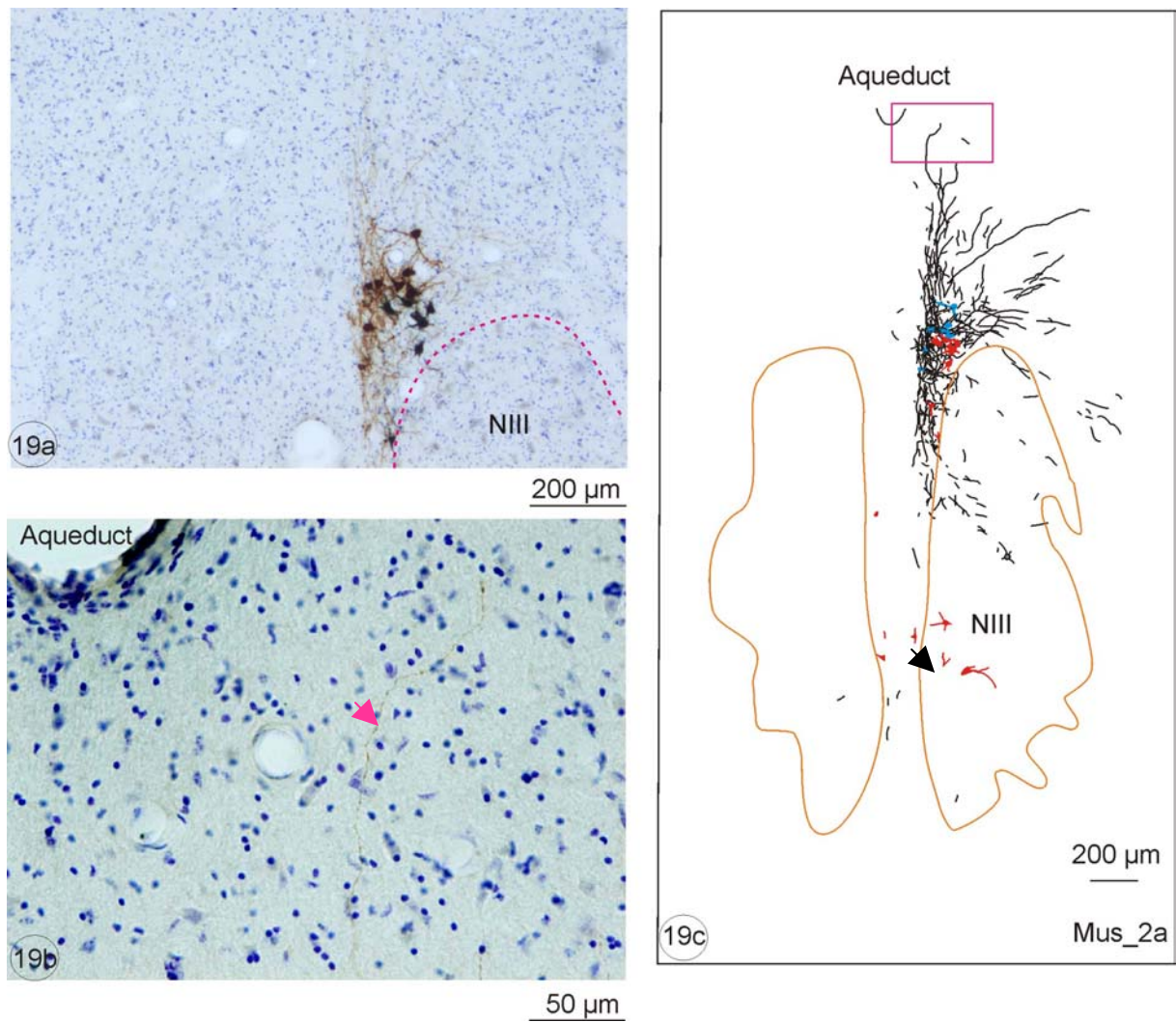


Fig. 19 Photographs and drawings of MIF motoneurons of MR and IR labelled by injection the tracer CTB and WGA-HRP into the distal tip of right MR and IR, respectively. 19a shows the group of labelled MR and IR MIF motoneurons which lie around the periphery of NIII. 19b is the detail of the frame in 19c under x20 magnification, showing the dendrites, which are close to the aqueduct (see the pink arrow head). 19c is the reconstructed figure of labelled neurons and dendrites. The red and blue parts represent the bodies of labelled IR and MR MIF motoneurons. The black arrow head shows that the labelled neurons were due to the tracer contamination of the IO. The SIF and MIF motoneurons of IO were both labelled with the tracer WGA-HRP.

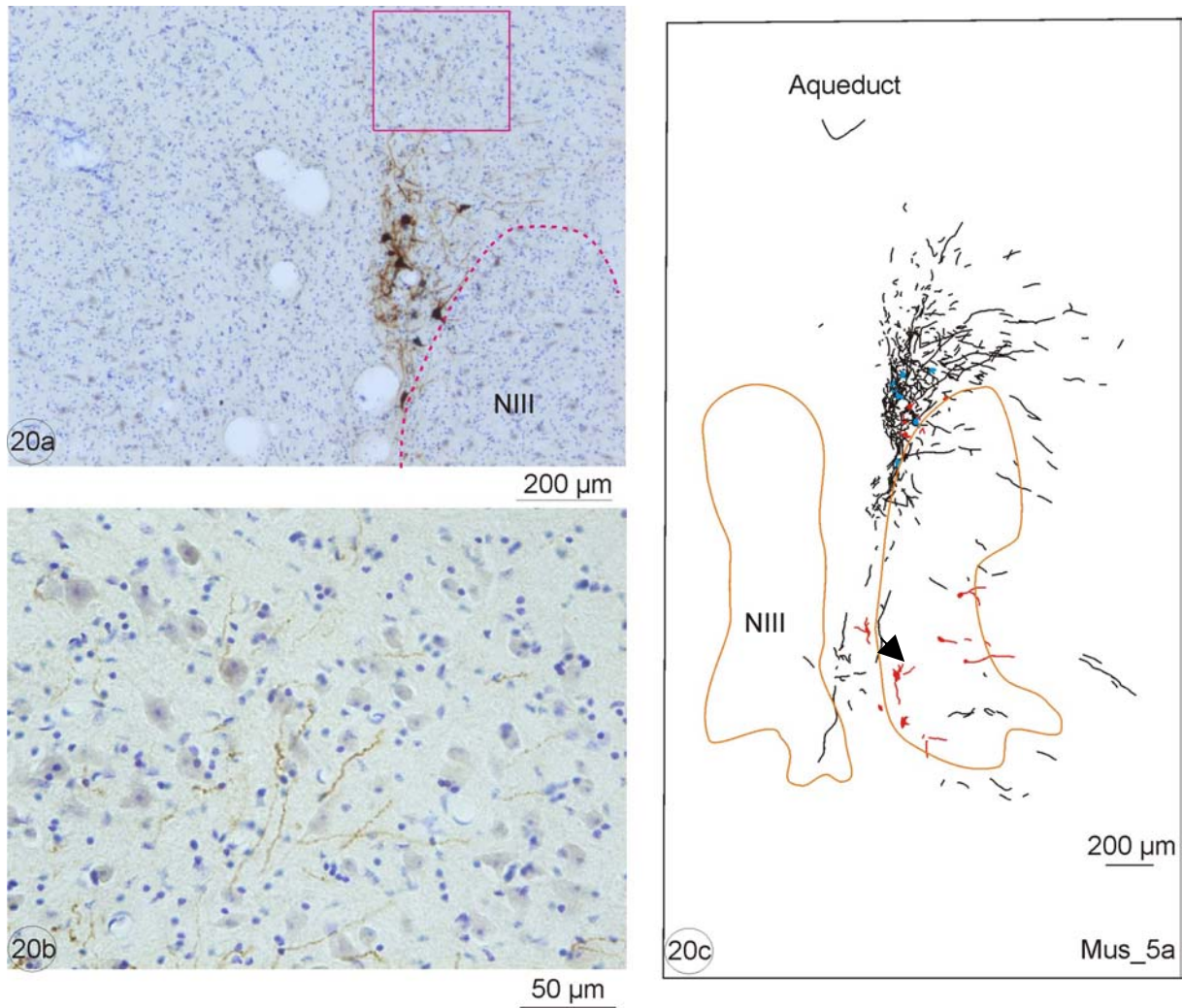


Fig. 20 Photographs and drawings of MIF motoneurons of MR and IR labelled by injection the tracer CTB and WGA-HRP into the distal tip of right MR and IR, respectively. 20a shows the group of labelled MR and IR MIF motoneurons which lie around the periphery of NIII. 20b is the detail of the frame in 20a under x20 magnification, showing the dendrites. 20c is the reconstructed figure of labelled neurons and dendrites. The red and blue parts represent the bodies of labelled IR and MR MIF motoneurons. The arrow head shows that the labelled neurons were due to the tracer contamination of the IO. The SIF and MIF motoneurons of IO were both labelled with the tracer WGA-HRP.

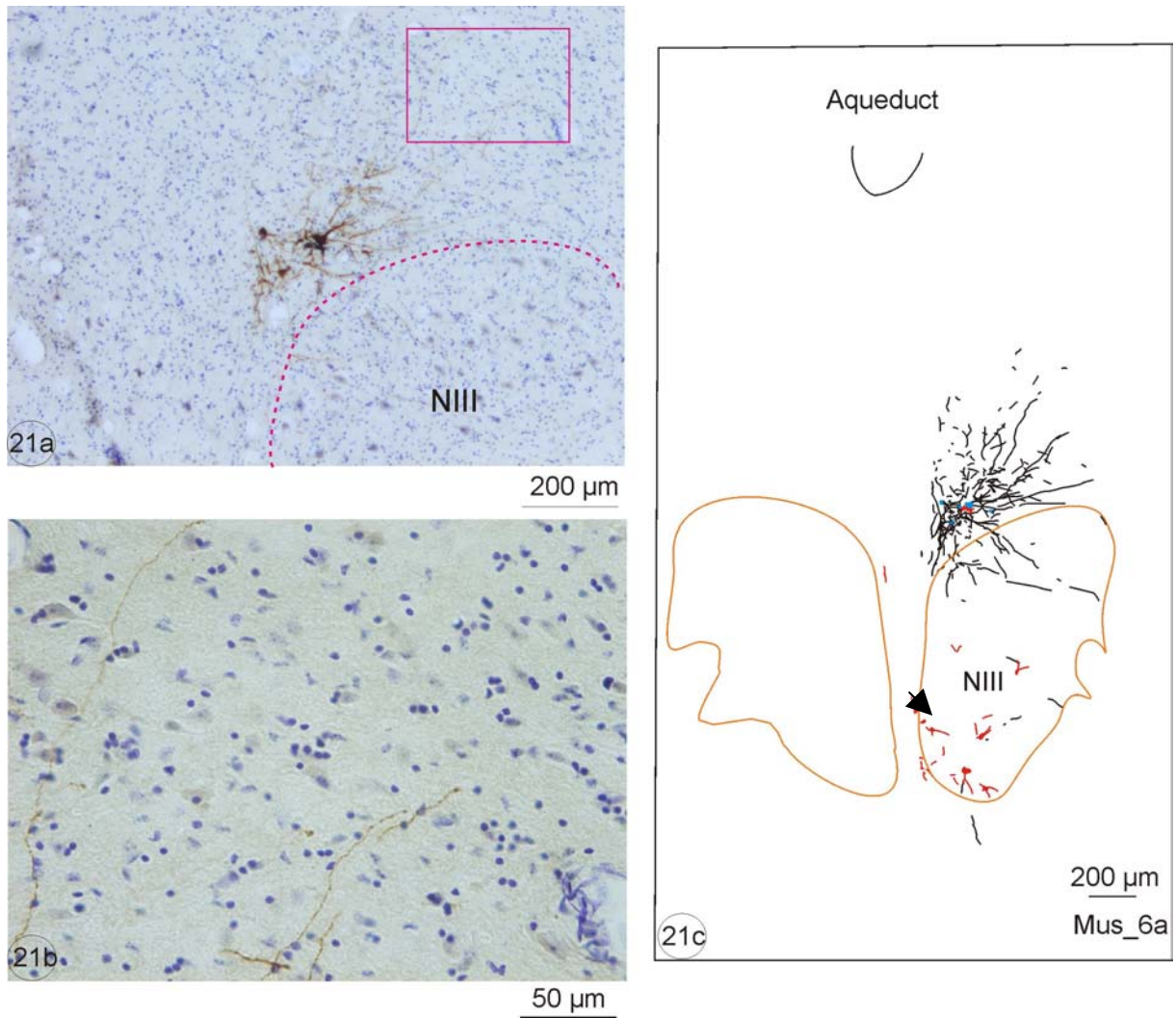


Fig. 21 Photographs and drawings of MIF motoneurons of MR and IR labelled by injection the tracer CTB and WGA-HRP into the distal tip of right MR and IR, respectively. 21a shows the group of labelled MR and IR MIF motoneurons which lie around the periphery of NIII. 21b is the detail of the frame in 21a under x20 magnification, showing the dendrites. 21c is the reconstructed figure of labelled neurons and dendrites. The red and blue parts represent the bodies of labelled IR and MR MIF motoneurons. The arrow head shows that the labelled neurons were due to the tracer contamination of the IO. The SIF and MIF motoneurons of IO were both labelled with the tracer WGA-HRP.

3.2.2 Distribution of the dendrites of IR MIF motoneurons in case B55

Since the dendritic pattern could be well demonstrated in CTB injection case, another case with a single CTB injection into IR was close to study. The tracer CTB injection into the distal tip of the right inferior rectus muscle resulted in the retrograde labelling of IR MIF motoneurons, non-twitch motoneurons, in the ipsilateral C-group, dorsomedial to the oculomotor nucleus (Fig. 22-25). The labelled neurons and dendrites were reconstructed (Fig. 22c, 23c, 24c, 25c).

The cell bodies lay dorsomedially to the classical oculomotor nucleus. The SIF and MIF motoneurons of IR lay adjacent to each other, so the IR MIF motoneuron group is not so separate when both are retrogradely labelled. One or two labelled neurons appeared on the middle line of NIII (marked by arrow head, Fig. 22c, 23c). This was attributed to the leakage of tracer CTB into the inferior oblique muscle.

The dendrites of IR MIF motoneurons radiated over a large area above the NIII, into the supraoculomotor area, but did not approach at the EW. The dendrites crossed the midline and spread into the opposite side (Fig. 22c, 24c, 25c). Generally, the dendrites of IR MIF motoneurons extended dorsally and bilaterally into the supraoculomotor area.

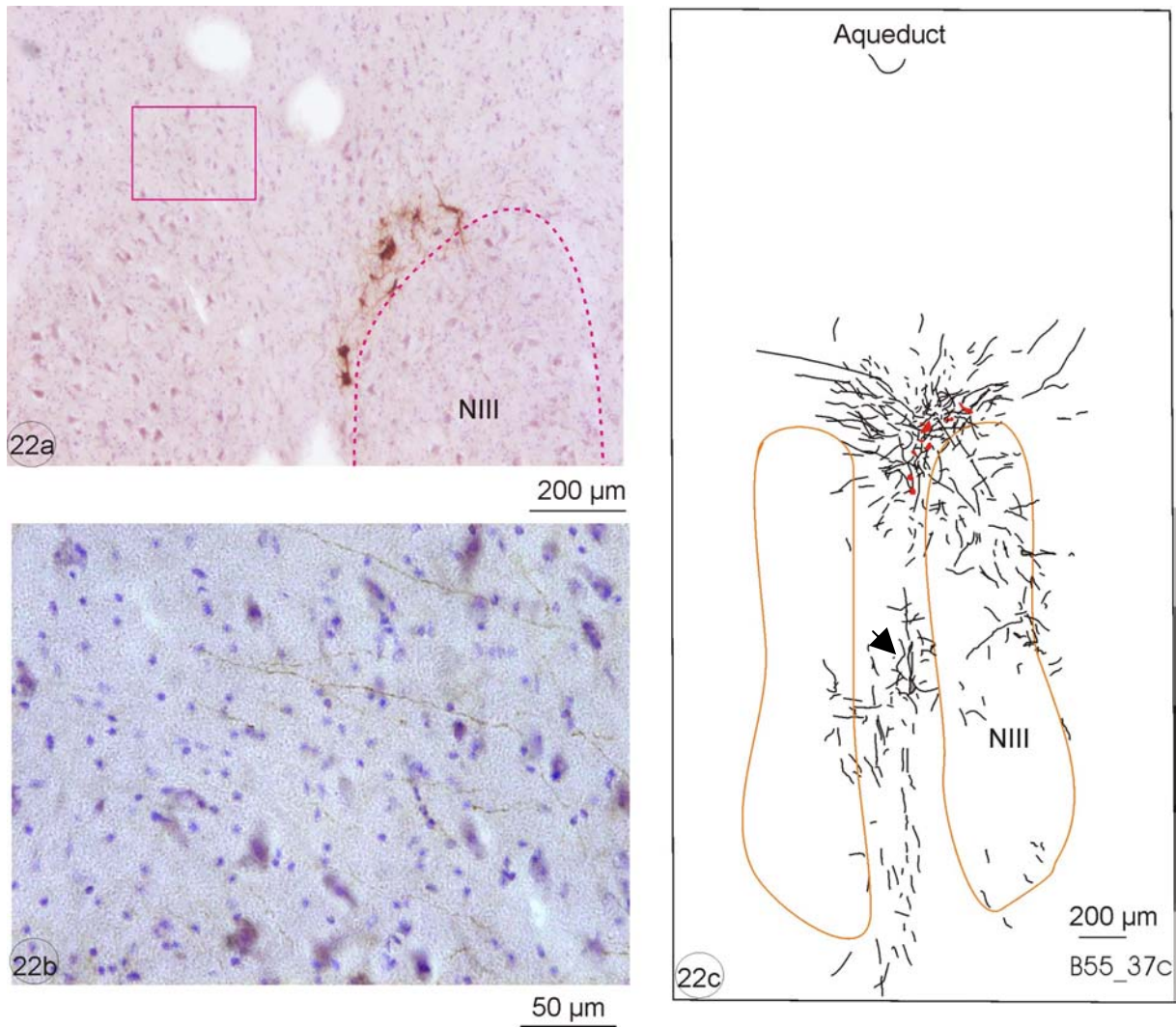


Fig. 22 Photographs and drawings of IR MIF motoneurons labelled by injection the tracer CTB into the distal tip of right inferior rectus muscle. 22a shows the group of IR MIF motoneurons which lie around the periphery of NIII. 22b is the detail of the frame in 22a under x20 magnification, showing the dendrites. 22c is the reconstructed figure of labelled neurons and dendrites. The red parts represent the cell bodies of labelled IR MIF motoneurons. The arrow head shows that IO motoneurons were labelled by leakage of tracer into the inferior oblique muscle.

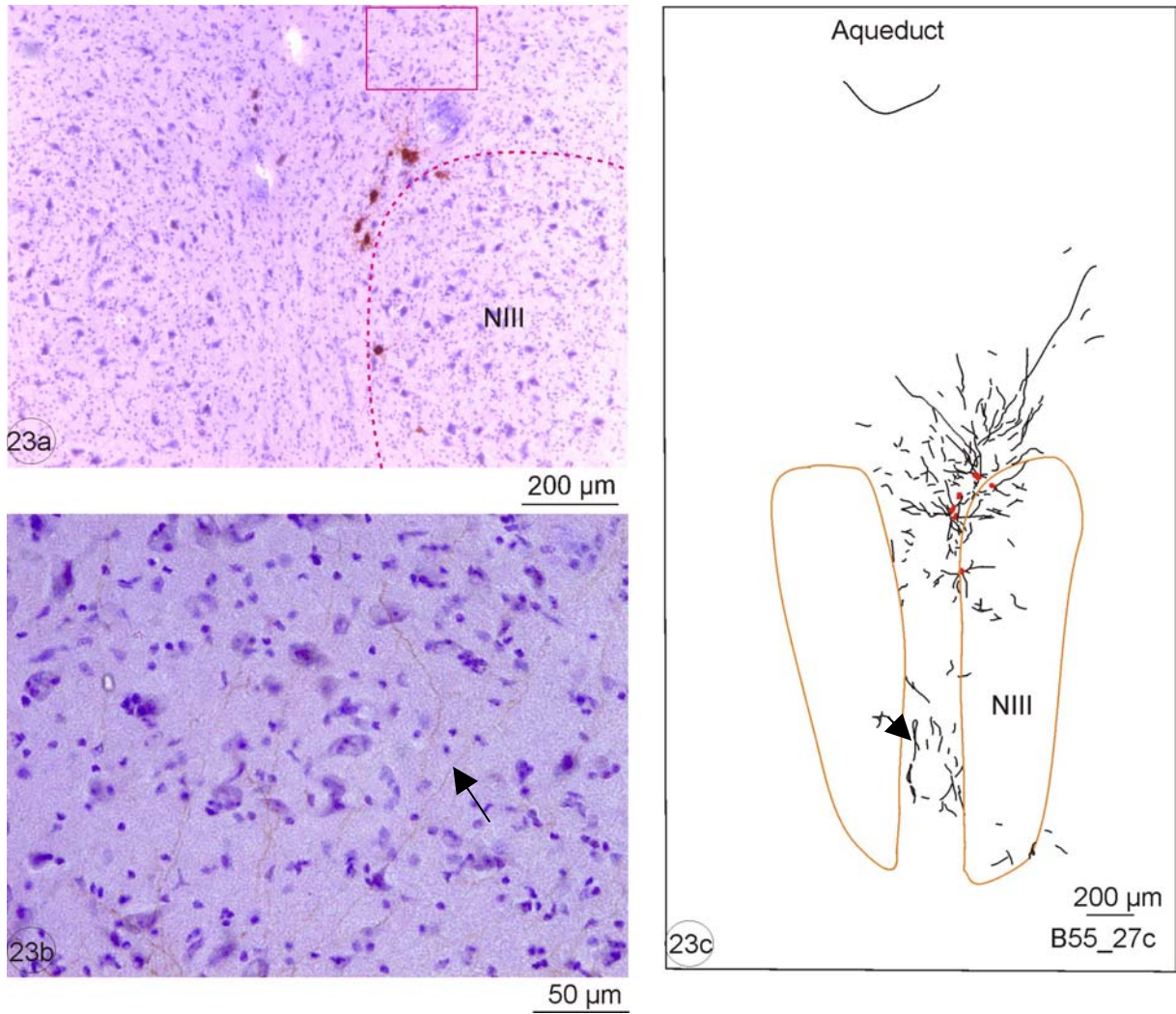


Fig. 23 Photographs and drawings of IR MIF motoneurons labelled by injection the tracer CTB into the distal tip of right inferior rectus muscle. 23a shows the group of labelled IR MIF motoneurons which lie around the periphery of NIII. 23b is the detail of the frame in 23a under x20 magnification, showing the dendrites (see the arrow). 23c is the reconstructed figure of labelled neurons and dendrites. The red parts represent the cell bodies of labelled IR MIF motoneurons. The arrow head shows that IO motoneurons were labelled by leakage of tracer into the inferior oblique muscle.

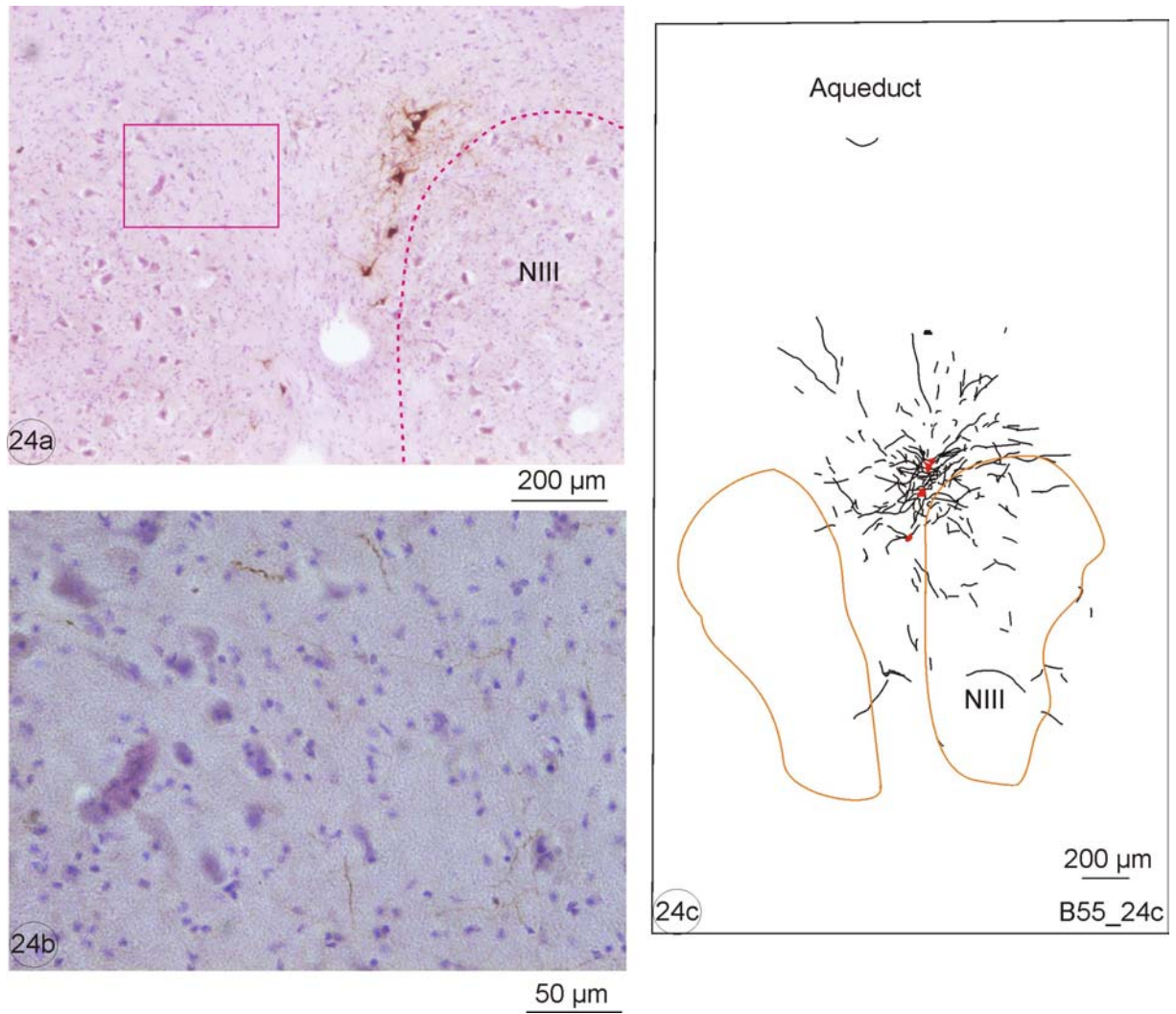


Fig. 24 Photographs and drawings of MIF motoneurons of IR labelled by injection the tracer CTB into the distal tip of right inferior rectus muscle. 24a shows the group of labelled IR MIF motoneurons which lie around the periphery of NIII. 24b is the detail of the frame in 24a under x20 magnification, showing the dendrites which extend into the opposite. 24c is the reconstructed figure of labelled neurons and dendrites. The red parts represent the cell bodies of labelled IR MIF motoneurons.

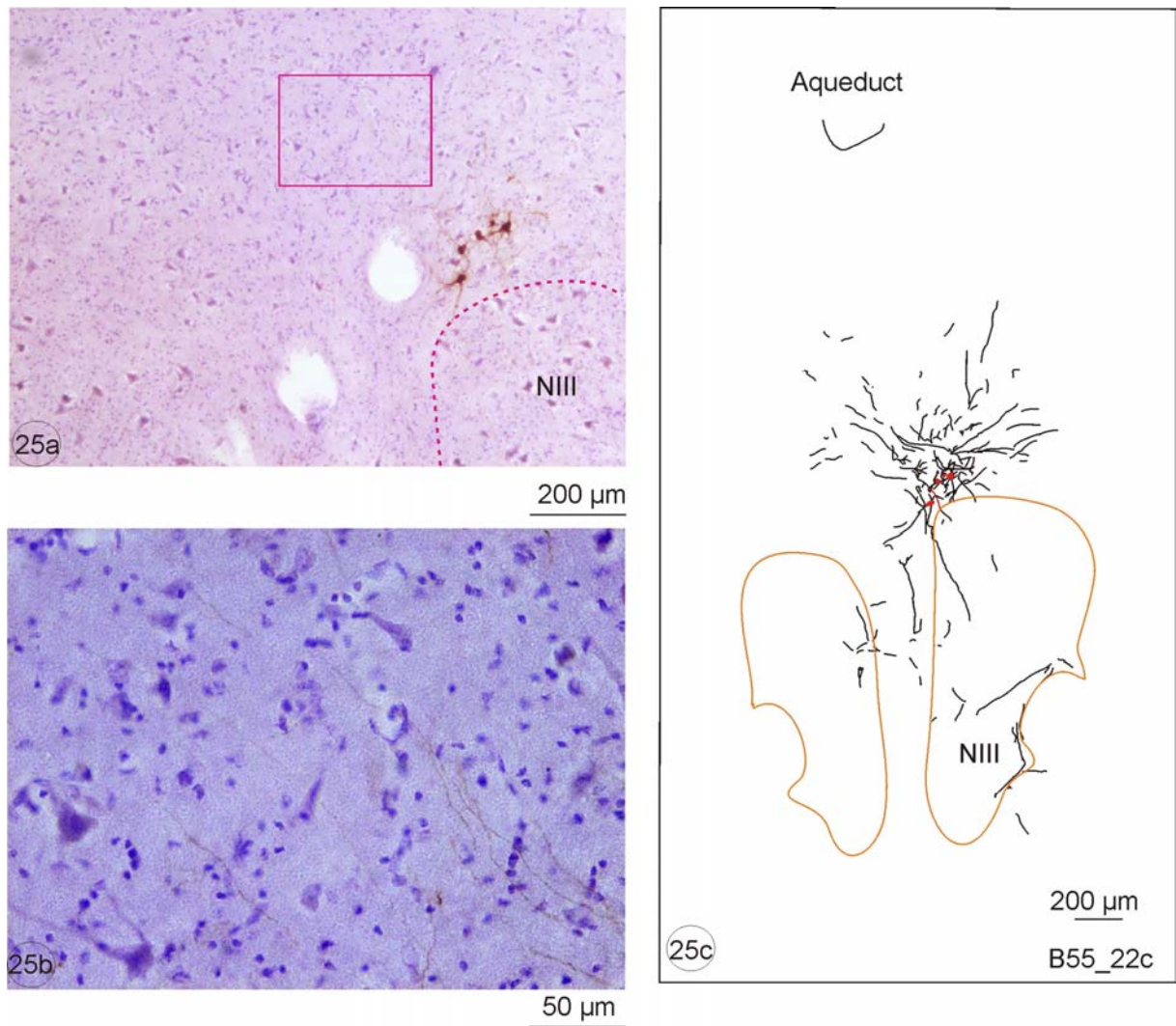


Fig. 25 Photographs and drawings of MIF motoneurons of IR labelled by injection the tracer CTB into the distal tip of right inferior rectus muscle. 25a shows the group of labelled IR MIF motoneurons which lie around the periphery of NIII. 25b is the detail of the frame in 25a under x20 magnification, showing the dendrites. 25c is the reconstructed figure of labelled neurons and dendrites. The red parts represent the cell bodies of labelled IR MIF motoneurons.

3.2.3 Comparison of MR and IR MIF motoneurons

1. There are no double-labelled MR and IR MIF motoneurons in C-group. So MR and IR MIF motoneurons are two different populations of MIF motoneurons in C-group.
2. From the result above, we found that the MIF motoneurons of MR and IR lay relatively separated to each other in the rostral two-thirds of NIII. The MR MIF motoneurons lay more dorsomedially, closer to midline than IR MIF motoneurons. There were more labelled MR MIF motoneurons than IR motoneurons in the rostral level of NIII. A few labelled neurons were close to the aqueduct in the rostral level of the oculomotor nucleus.
3. The dendrites of MR MIF motoneurons extended to supraoculomotor area and penetrated into the Edinger-Westphal nucleus ipsilaterally. In contrast, the dendrites of IR MIF motoneurons spread bilaterally into the supraoculomotor area, but did not approach the Edinger-Westphal nucleus.

4 Discussion

Our results demonstrate the relative location of the MR and IR MIF motoneurons in C-group simultaneously labelled by two retrograde tracers WGA-HRP and CTB. In summary, they showed that there are no double-labelled MR and IR MIF motoneurons in C-group. They lie relatively separated in the dorsomedial part of the oculomotor nucleus. The MR MIF motoneurons lie more dorsomedially than IR MIF motoneurons. The dendritic spread of MR and IR MIF motoneurons also differed. The dendrites of MR MIF motoneurons extend high into the SOA, involving the Edinger-Westphal nucleus, ipsilaterally. A few of these motoneurons even lie further dorsally than EW. In contrast to MR MIF motoneurons, the dendrites of IR MIF motoneurons spread into the supraoculomotor area, not approach the EW, but bilaterally.

We will discuss the functional implications of these properties of the medial and inferior recti MIF motoneurons and the two tracers that were used in this study.

4.1 Location of MIF motoneurons in the oculomotor nucleus

The results of these experiments are consistent with previous study (Büttner-Ennever et al., 2001). A distal tracer injection into the myotendinous junction of extraocular muscles, which targets primarily the global layer in primates (Demer et al., 2000; Oh et al., 2001), labels mainly the MIF motoneurons around the periphery of the classical oculomotor nucleus. However a few scattered neurons could often be found within the boundaries of the NIII as well. The motoneurons of SIFs and MIFs lie separated from each other in NIII and have a completely different organization of their subgroups, and different inputs (Büttner-Ennever and Akert, 1981; Wasicky et al., 2004). Our experiments show that MIF motoneurons of MR are located more dorsomedially, and closer to midline than IR MIF motoneurons, specially in the rostral level of oculomotor nucleus (Fig. 14). Eberhorn et al., (2005) showed that the complete population of motoneurons (including SIF and MIF motoneurons) in SOA and NIII can be visualized by ChAT-immunolabelling in monkey (Fig. 26). The C-group motoneurons extended dorsally deep into SOA. The total extent of C-group motoneurons is more than what we retrogradely labelled in this experiment, but the labelled neurons can qualitatively represent the general character of MIF motoneurons in the C-group. The dendrites of MR MIF motoneurons extend into SOA and EW ipsilaterally. While the IR MIF motoneurons dendrites spread bilaterally into SOA, but not approach at the EW. In general, the dendrites of MIF

motoneurons extend much further into the SOA than the dendrites of SIF motoneurons (see Fig. 26). A more accurate estimation could be made from an intracellular injection study.

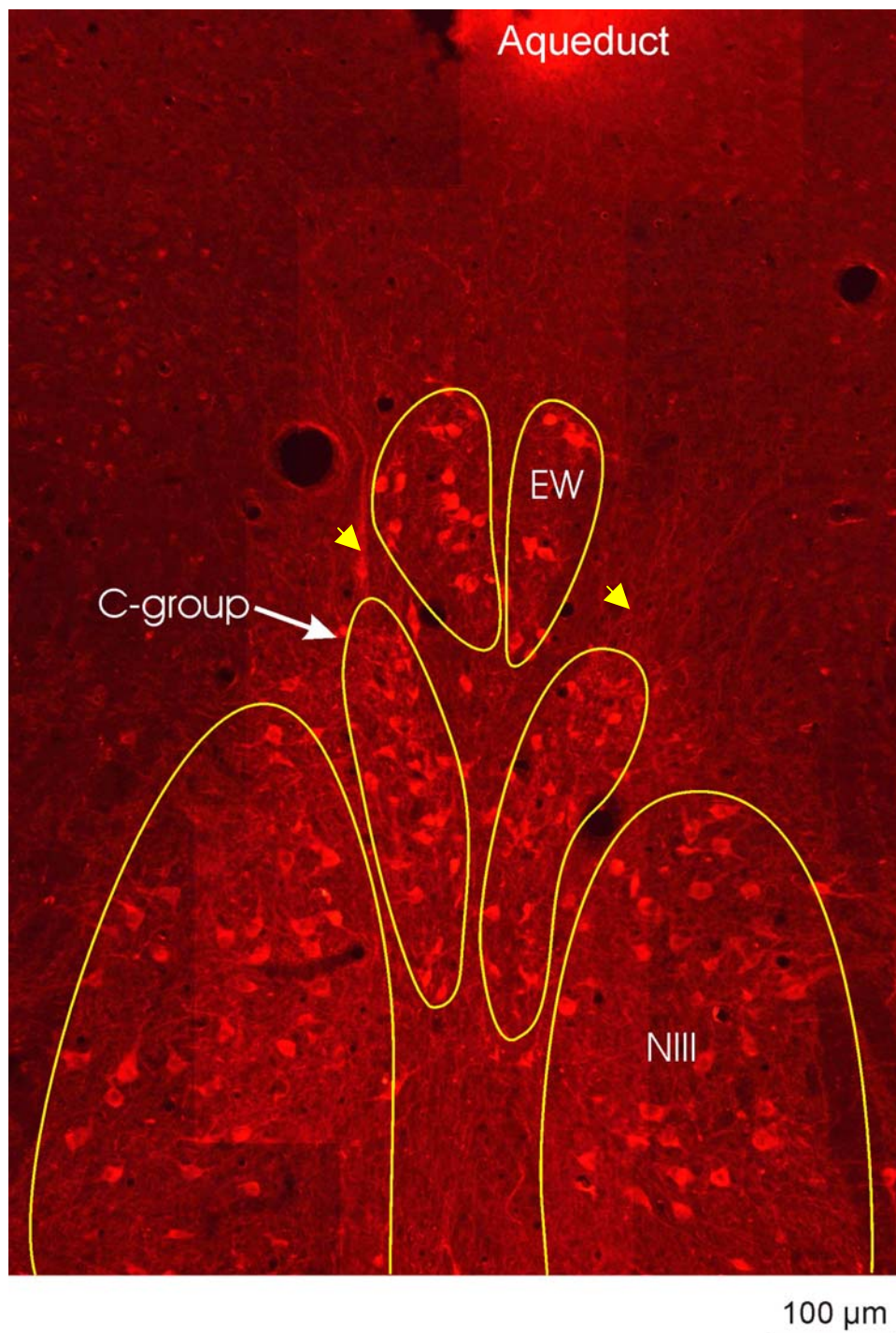


Fig. 26 Photograph of the complete population of motoneurons (SIF and MIF motoneurons) which were visualized by ChAT-immunolabelling in supraoculomotor area and NIII in Monkey. The drawings in the picture show the boundary of EW, C-group and NIII. The complete C-group motoneurons (pointed by arrow) occupied the space between the NIII and EW. The yellow arrow head show that the dendrites of C-group non-twitch motoneurons extend into the SOA (Adapted from Eberhorn AC, et al., 2005).

4.2 Tracer properties

Cholera toxin subunit B is a well-known retrograde tracer in the central nervous system. It was retrogradely transported to the neuronal cell bodies and produced a Golgi like image of the labelled neurons, as CTB can be detected throughout the neuronal cytoplasm, in proximal dendrites and even in distal dendrites and axons (Ericson and Blomqvist, 1988; Llewellyn-Smith et al., 1992). Several studies showed that CTB is a more sensitive retrograde tracer than WGA and WGA-HRP in the central nervous systems of cats and rats, but not in the peripheral nervous system (Luppi et al., 1990; Peyron et al., 1998). In addition, CTB is taken up and transported in damaged, but not in intact fibres passage, so spillage and uptake from surrounding area must be taken into account. CTB can be applied iontophoretically to study the afferents to small cell groups without any evidence of tissue necrosis in the injection sites and therefore very little artefactual labelling due to uptake by damaged fibers of passage (Luppi et al., 1990). In this study, SIF motoneurons of the injected muscle or other eye muscles of the same orbit may be involved (see Fig.22c, 23c). CTB is quite stable after it has reached the neuronal cell body and can be detected in neurons for several weeks after injection (Leman et al., 2000). Paraformaldehyde fixative is ideal for CTB. The labelled neurons can be well revealed by light microscopy as in our studies, but for the electron microscopy, caution must be taken because CTB is sensitive to the glutaraldehyde fixative (Llewellyn-Smith et al., 1992). CTB also can be used as an anterograde tracer with particular immunocytochemical procedures (Angelucci et al., 1996). In this study, we used CTB as the retrograde tracer, which was injected into the distal tip of eye muscles to trace the motoneurons that innervate the eye muscles. In case B55, tracer was taken up by the MIF motoneurons which innervate the inferior rectus, but also taken up by few motoneurons which innervate the inferior oblique muscle.

WGA-HRP is the other tracer used in our experiments. It is a sensitive bi-directional tracer. It can be retrograde and anterograde transported, resulting in the anterograde labelling of axon terminals and retrograde labelling of cell bodies. Gonatas et al., (1979) first described that HRP conjugated with the lectin WGA as an axonal tracer can improve sensitivity 40 times greater than free HRP. So WGA-HRP has become the most widely used neuroanatomical tracers. It is not only used for studies of central nervous system connection at the light microscope level, but also in studies of ultrastructural detail (Teune et al., 1998). It has also proven to be an effective transneuronal tracer, permitting studies of multisynaptic pathways (Krug et al., 1998). The retrograde and anterograde transport rates WGA-HRP are quite

different. The anterograde transport rates are thought to exceed 300mm/day, while retrograde rates are in the order of 100mm/day (Mesulam, 1982; Gibson et al., 1984). The transport rate can be influenced heavily by other factors, including uptake time and choice of anaesthetic. It is known that pentobarbitone can inhibit the transport of HRP (Mesulam and Mufson, 1980). Survival time also can affect the WGA-HRP labelling. Trott and Apps (1993) found that survival time of less than 2 days fails to produce any detectable retrograde labelling in the inferior olive after injection of WGA-HRP into the cerebellar cortex. By contrast, periods in excess of 5 days are considered likely to result in transneuronal labelling and an inaccurate estimation of the size of the effective injection site, as well as some decrease in labelling (Gibson et al., 1984; Mesulam, 1982). In our studies, the survival time was 3 days which exclude any WGA-HRP transneuronal labelling. Unlike free HRP, WGA-HRP is not thought to be taken up by intact fibres passing through the injection site (Brodal et al., 1983). Using the highly sensitive chromogen Tetramethylbenzidine (TMB) (Mesulam, 1978) as a substrate for horseradish peroxidase histochemistry is a traditional neuronal tracing method. But the TMB method has a number of disadvantages. The duration of storage, the perfusion, composition of storage medium, the type of counterstaining and the dehydration process can affect the TMB reaction (Mesulam and Mufson, 1980). Overreaction with TMB can produce crystals that extend beyond the membranous boundaries of neurons (Gong and LeDoux, 2003). WGA-HRP is also highly diffusible neuronal tracer (Köbbert and Thanos, 2000). This is why we got leakage into the IO in the first case MUS (see arrow head Fig.17c, 18c, 2a, 5a, 6a). Traditional histochemical detection of wheat germ agglutinin-horseradish peroxidase can impose substantial technical limitations on studies requiring co-localization of neurotransmitters, receptors and other neural antigens. Recently anti-WGA, anti-HRP antibodies were used for detecting the WGA-HRP (Gong and LeDoux, 2003). Compared to the traditional histochemical detection methods, the immunohistochemical detection of WGA-HRP has several advantages. For example, first, there is no special requirement for the tissue fixation. Second, unconjugated WGA can be used as the neuroanatomical tracer since WGA may be a more sensitive tracer than WGA-HRP (Ruda and Coulter, 1982; Horikawa and Powell, 1986). Third, a wide variety of detection methods can be used for the detection of WGA-HRP, so allowing for the co-localization of several other markers and increasing experimental flexibility when using multiple tracers in the same animal. After detection of WGA or HRP with unconjugated primary antibodies, tracer can then be visualized with biotin-, colloidal gold- or fluorochrome-tagged secondary antibodies.

In a comparison of CTB and WGA-HRP, Behzadi et al., (1990) reported that CTB recognized by immunohistochemistry is a much more sensitive tracer in the central nervous systems than WGA-HRP revealed by the TMB method. But WGA-HRP can be visualized by immunohistochemical technique which is much more sensitive than traditional TMB method (Gong and LeDoux, 2003). In this study, WGA-HRP was visualized by TMB method. The cell bodies are well labelled, but the dendrites are not so far or fully labelled as CTB staining. So we only compared the CTB labelled IR MIF motoneurons group in case B55 with CTB labelled MR MIF motoneurons in case MUS.

4.3 The function of C-group motoneurons in vergence eye movements

Supraoculomotor area is the part of the periaqueductal gray located immediately above the oculomotor nucleus. Laterally it is continuous with the mesencephalic reticular formation. The SOA receives projections from the superior colliculus (Edwards and Henkel, 1978), two deep cerebellar nuclei (the posterior interposed nucleus and the fastigial nucleus) (May et al., 1992), the pretectum (Büttner-Ennever et al., 1996b), the accessory optic nuclei (Blanks et al., 1995). Direct projections from the frontal and supplementary eye fields to the SOA have also been traced (Stanton et al., 1988; Shook et al., 1990), as well as two regions of the cerebral cortex where vergence responses have been recorded (Gamlin and Yoon, 2000; Fukushima et al., 2005). Several studies indicate that the connectivity of MLF and abducens internuclear neurons to MR and its neural activity do not play an important role in vergence eye movements. Internuclear ophthalmoplegia, characterized by damage of the medial longitudinal fasciculus (MLF) that interrupts the abducens internuclear neurons excitatory pathway shows loss of conjugate adduction on the side of lesion, but adduction for vergence is spared. In contrast, certain midbrain lesions cause vergence deficits, but sparse conjugate eye movement (reviewed by Leigh and Zee, 1999). In primates, both abducens motoneurons and internuclear neurons decrease their firing rate during convergence (Mays and Porter, 1984; Gamlin et al., 1989a). Miller et al., (2002) found LR force missing and MR co-contraction absent in ocular convergence. Therefore, there must be another powerful (excitatory) vergence input to MR motoneurons. It is possible that SOA might provide this excitatory signal (Mays and Porter, 1984).

Other experiments have shown that the SOA and the adjacent reticular formation around the oculomotor nucleus contain premotor neurons related to vergence eye movement in

monkeys (Mays and porter, 1984; Judge and Cumming, 1986; Zhang et al., 1992). Three main types of neurons can be found in the SOA: those that discharge in relation with vergence angle (vergence tonic cells), to vergence velocity (vergence burst cells), and both to vergence angle and velocity (vergence tonic-burst cells) (Leigh and Zee, 2006). Many of these cells also discharge with accommodation, but they carried a signal predominantly related to vergence. These neurons increase the firing rate for near viewing, but not during vertical or horizontal conjugate eye movement. Mays (1984) suggested that the output of midbrain near response cells might provide the vergence command needed by the medial rectus motoneurons. It has been proved that the medial rectus subdivision of the oculomotor nucleus get a direct projection from the neurons in the vicinity of the oculomotor nucleus by the antidromic microstimulation techniques in anesthetized, paralyzed cats (Nakao et al., 1986). Zhang et al., (1991) also has shown that numbers of near response cells can be antidromically activated by microstimulation of the ipsilateral medial rectus subdivision of the oculomotor nucleus, but in these experiments they failed to activate near response cells from the contralateral oculomotor nucleus. They suggested that vergence input to medial rectus motoneurons may be mainly ipsilateral. Our results show that the dendrites of MR MIF motoneurons spread only ipsilaterally into the SOA. Anatomically this supports the concept that the MR MIF motoneurons get vergence input ipsilaterally and may also participate vergence eye movements. Unfortunately until now, there have been no known recording from MIF motoneurons in the awake animal to identify their functional properties, apart from one study in the frog where the neuronal activity was tonic and correlated with intended eye position (Dieringer and Precht, 1986). Up to now, single-cell recordings from the behaving monkeys show that all extraocular motoneurons participate in all types of eye movement: vergence, saccade, smooth pursuit, vestibulo-ocular reflex and optokinetic nystagmus. However, it is not clear how much the MIF motoneurons contribute to the tension of eye movement, but experimentally exposing eye muscle to succinylcholine causes them to contract and the effect is caused by the depolarization of MIFs and not SIFs (Bach-y-Rita et al., 1977).

4.4 Relationship of C-group motoneurons with Edinger-Westphal nucleus

The Edinger-Westphal nucleus, anteromedian nucleus and adjacent neurons in the ventral tegmental area (VTA) are sources of preganglionic parasympathetic innervation of intraocular smooth muscle, including pupillary muscle, the ciliary body and blood vessels in mammals

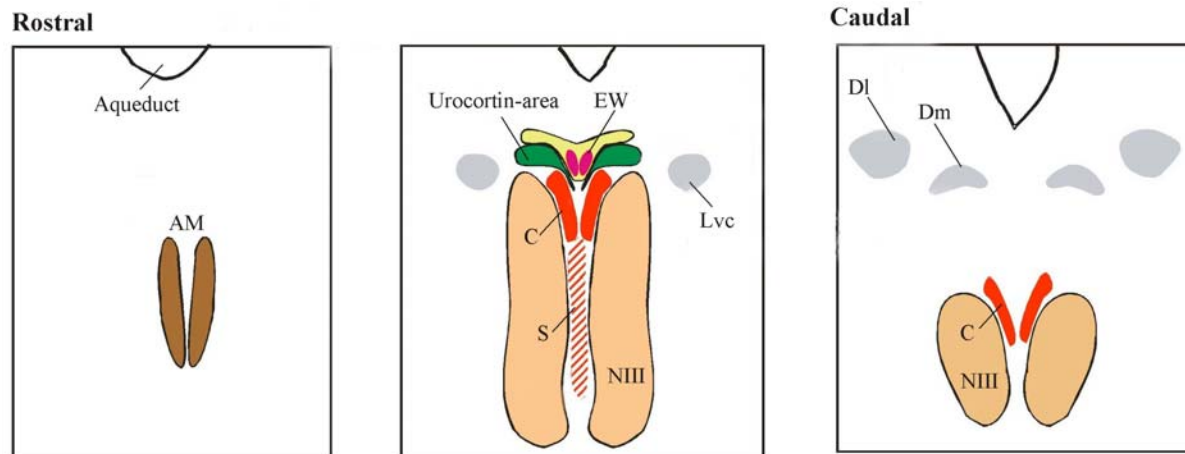


Fig. 27 The schematic drawing of the supraoculomotor area from rostral to caudal in monkey. The supraoculomotor area contains three main groups: AM; Urocortin-area (supraoculomotor area containing urocortin-positive neurons) and EW. The AM contains preganglionic neurons. The EW in monkey, medial magnocellular group, contains the cholinergic preganglionic neurons. The Urocortin-area contains a large group of urocortin-positive neurons which lie ventrolaterally to the large cholinergic preganglionic neurons. The C-group is the MIF motoneurons which innervated the MR and IR global layer. The S-group is the MIF motoneurons which innervated the SR and IO global layer. Dl is dorsolateral area, Dm is dorsomedial area. (Adapted from Horn-Bochtler AK et al., 2006 Neuroscience meeting, poster 345. 9/S4)

(Balaban, 2003). The parasympathetic preganglionic neurons project ipsilaterally via the oculomotor nerve to the ciliary ganglion, which innervates the sphincter pupillary muscle of the iris for pupillary constriction and ciliary body for lens accommodation (Narayanan and Narayanan, 1976; Lyman and Mugnaini, 1980). In birds, the neurons in the ciliary ganglion that innervate the iris sphincter muscle and the ciliary body receive input specifically from cells in the lateral EW, whereas those that innervate choroidal blood vessels receive input from cells in the medial EW (Reiner et al., 1983; Gamlin et al., 1984). Gamlin and Reiner (1991) have identified another two inputs to the avian EW, the medial mesencephalic reticular formation and rostral lateral mesencephalic reticular formation. In cats and rabbits, the preganglionic neurons are in a completely different location, neither in the EW, nor in AM. Instead the preganglionic neurons lie in the ipsilateral rostral periaqueductal region dorsal to the NIII, and the tegmentum ventral to the oculomotor complex (Loewy and Saper, 1978; Sugimoto et al., 1977; Strassman et al., 1987; Tozoshima et al., 1980; Maciewicz, 1983; Erichsen and May, 2002). The pupil-related preganglionic motoneurons are located rostrally, in and lateral to the anteromedian nucleus. In contrast, the lens-related preganglionic motoneurons are particularly prevalent caudally, both dorsal and ventral to the oculomotor

nucleus (Erichsen and May, 2002). In monkey, the preganglionic neurons are largely confined to EW and AM (Akert et al., 1980; Burde and Loewy, 1980; Ishikawa et al., 1990; May et al., 1992; Sun and May, 1993), but some reports found cells lateral to EW in the lateral visceral cell columns (Lvc) of the ventrolateral periaqueductal gray (Burde and Williams, 1989) (Fig. 27). Horn-Bochtler et al., (2006) investigated the histochemical properties of these groups in the monkey, and delineated the cholinergic EW proper, the anteromedian nucleus and MIF motoneurons of the oculomotor nucleus, along with adjacent non-cholinergic cell groups. The EW area is one of the major cellular urocortin expressing sites in the rat brain (Spina et al., 2004). Urocortin-positive areas are thought to be involved in the acute stress and feeding behavior (Kozicz, 2003). But in monkey the urocortin expressing site lies ventrolaterally to the large cholinergic preganglionic neurons. The function of EW includes a control of the “near response” or “near triad” which comprises three elements: pupillary constriction and accommodation, vergence (Leigh and Zee, 1999). The first two functions are controlled by EW neurons around the dorsomedial of the NIII, which is occupied by C-group MIF motoneurons (Fig. 27).

The EW nucleus get direct projections from only one retinorecipient pretectal nucleus, the pretectal olivary nucleus whose physiology is appropriate for mediating the pupillary light reflex (Gamlin and Clarke, 1995; Gamlin, 2005). Clarke et al., (2003) found that in marmoset, the pretectal olivary nucleus connects with the preganglionic neurons in the EW nucleus as well as with the lateral terminal nucleus, which in turn also connects with the EW nucleus. A major input to the MIF motoneurons of the C- and S-groups is the pretectum (Büttner-Ennever et al., 1996).

May et al., (1992) found out that the midbrain near-response region has reciprocal anatomic connections with two deep cerebellar nuclei, the posterior interposed nucleus and the fastigial nucleus. The projection from two deep cerebellar nuclei is predominantly contralateral, whereas the projection to the deep nuclei predominantly is ipsilateral. Neurons in the posterior interposed nucleus projected to the SOA but not Edinger-Westphal nucleus. But fastigial nucleus neurons project to both the SOA and EW. The activity of neurons in the posterior interposed nucleus and fastigial nucleus is related to the “far-response” and “near-response” respectively (Zhang and Gamlin, 1998). Furthermore, some recent clinical findings reported that deficits in accommodation are associated with cerebellar lesion (Kawasaki et al., 1993). From our experiment, we can not prove that C-group MIF motoneurons contact the neurons in EW, but the dendrites of MR MIF motoneurons do extend into the EW and SOA. It has been proved that the smaller distal dendrites of C-group MIF motoneurons receive most of the

synaptic input (May et al., 2000). Much of these synaptic inputs to the C-group neurons is provided by inputs to EW suggests that these neurons may be driven by accommodation signals. There are a few labelled MIF motoneurons of C-group located around the EW, close to the periaqueductal gray. The C-group MIF motoneurons and EW both receive input from the pretectum. Lens accommodation ordinarily accompanies convergence. The model of vergence and accommodation are suggested to be cross-coupled (Zhang et al., 1992). These data all support the hypothesis that C-group motoneurons and EW receive a similar premotor input and all participate in the near response for vergence and accommodation. This result confirms Gamlin's suggestion that both EW neurons and medial rectus motoneurons receive input from near-response neurons which are related with both vergence and accommodation. Microstimulation at the sites of EW neurons produced accommodation in the ipsilateral eye, but there are few neurons in EW which showed some activity related to vergence (Gamlin et al., 1994). The labelled MR MIF motoneurons which lie around the EW, and are close to the periaqueductal gray might explain why few neurons in EW showed some activity related to vergence.

5 Conclusions

1. The present work demonstrates that MR and IR MIF motoneurons are two populations of neurons in C-group. There is no neuron in C-group projecting to both medial rectus and inferior rectus muscles.
2. The MR and IR MIF motoneurons lie relatively separated in the rostral two-thirds of NIII. The MR MIF motoneurons lie more dorsomedially, closer to midline than IR MIF motoneurons. Some of the labelled MR MIF motoneurons are located around EW. This suggests that MR MIF motoneurons might receive the same input as EW which plays a role in the “near response”.
3. The dendrites of MR MIF motoneurons spread into SOA and EW ipsilaterally, in contrast, IR MIF motoneurons’ dendrites ramified into SOA, bilaterally. This result qualitatively suggests that MR and IR MIF motoneurons might have different function in the eye movements.
4. These results support the hypothesis that IR MIF motoneurons may contribute to the eye alignments, along with MIF motoneurons of other eye muscles. But MR MIF motoneurons appear to be different and may also participate the vergence eye movements.

6 Literature cited

Angelucci A, Clasca F, Sur M. 1996. Anterograde axonal tracing with the subunit B of cholera toxin: a highly sensitive immunohistochemical protocol for revealing fine axonal morphology in adult and neonatal brains. *J Neurosci Methods* 65:101-12.

Akert K, Glicksman MA, Lang W, Grob P, Huber A. 1980. The Edinger-Westphal nucleus in the monkey. A retrograde tracer study. *Brain Res* 184:491-8.

Alvarado-Mallart RM, Pincon-Raymond M. 1979. The palisade endings of cat extraocular muscles: a light and electron microscope study. *Tissue Cell* 11:567-84.

Bach-y-Rita P, Lennerstrand G, Alvarado J, Nichols K, McHolm G. 1977. Extraocular muscle fibers: ultrastructural identification of iontophoretically labeled fibers contracting in response to succinylcholine. *Invest Ophthalmol Vis Sci* 16:561-5

Balaban CD. 2003. Vestibular nucleus projections to the Edinger-Westphal and anteromedian nuclei of rabbits. *Brain Res* 963:121-31.

Blanks RH, Clarke RJ, Lui F, Giolli RA, Van Pham S, Torigoe Y. 1995. Projections of the lateral terminal accessory optic nucleus of the common marmoset (*Callithrix jacchus*). *J Comp Neurol* 354:511-32.

Behzadi G, Kalen P, Parvopassu F, Wiklund L. 1990. Afferents to the median raphe nucleus of the rat: retrograde cholera toxin and wheat germ conjugated horseradish peroxidase tracing, and selective D-[3H] aspartate labelling of possible excitatory amino acid inputs. *Neuroscience* 37:77-100.

Bondi AY, Chiarandini DJ. 1983. Morphologic and electrophysiologic identification of multiply innervated fibers in rat extraocular muscles. *Invest Ophthalmol Vis Sci* 24:516-9.

Brodal P, Dietrichs E, Bjaalie JG, Nordby T, Walberg F. 1983. Is lectin-coupled horseradish peroxidase taken up and transported by undamaged as well as by damaged fibers in the central nervous system? *Brain Res* 278:1-9.

Brooke MH, Kaiser KK. 1970. Muscle fiber types: how many and what kind? *Arch Neurol* 23:369-79.

Burde RM, Loewy AD. 1980. Central origin of oculomotor parasympathetic neurons in the monkey. *Brain Res* 198: 434-439.

Burde RM, Williams F. 1989. Parasympathetic nuclei. *Brain Res* 498:371-5.

Burke RE. 1981. Motor units: anatomy, physiology and functional organization. In: *Handbook of physiology, Section 1, The nervous system, Vol II, Motor systems* (Brooks VB, ed) pp 345-422.

Büttner-Ennever JA, Akert K. 1981. Medial rectus subgroups of the oculomotor nucleus and their abducens internuclear input in the monkey. *J Comp Neurol* 197:17-27.

Büttner-Ennever JA, Cohen B, Horn AK, Reisine H. 1996. Pretectal projections to the oculomotor complex of the monkey and their role in eye movements. *Comp Neurol* 366:348-59.

Büttner-Ennever JA, Horn AK, Scherberger H, D'Ascanio P. 2001. Motoneurons of twitch and nontwitch extraocular muscle fibers in the abducens, trochlear, and oculomotor nuclei of monkeys. *J Comp Neurol* 438:318-35.

Büttner-Ennever JA. 2006. The extraocular motor nuclei: organization and functional neuroanatomy. *Prog Brain Res* 151:95-125.

Clarke RJ, Alessio ML, Pessoa VF. 1987. Distribution of motoneurons innervating extraocular muscles in the brain of the marmoset (*Callithrix jacchus*). *Acta Anat (Basel)* 130: 191-6.

Clarke RJ, Blanks RH, Giolli RA. 2003. Midbrain connections of the olivary pretectal nucleus in the marmoset (*Callithrix jacchus*): implications for the pupil light reflex pathway. *Anat Embryol (Berl)* 207:149-55.

Dean P. 1996. Motor unit recruitment in a distributed model of extraocular muscle. *J Neurophysiol* 76:727-42.

Demer JL, Oh SY, Poukens V. 2000. Evidence for active control of rectus extraocular muscle pulleys. *Invest Ophthalmol Vis Sci* 41:1280-90.

- Demer JL. 2002. The orbital pulley system: a revolution in concepts of orbital anatomy. *Ann N Y Acad Sci* 956:17-32.
- Dieringer N, Precht W. 1986. Functional organization of eye velocity and eye position signals in abducens motoneurons of frog. *J Comp. Physiol* 158:179-194.
- Dogiel AS. 1906. Die Endigungen der sensiblen Nerven in den Augenmuskeln und deren Sehnen beim Menschen und den Säugetieren. *Arch. Mikrosk. Anat* 68:501-526.
- Duncan JE, Goldstein LS. 2006. The genetics of axonal transport and axonal transport disorders. *PloS Genet.* 2:e124.
- Eberhorn AC, Ardeleanu P, Büttner-Ennever JA, Horn AK. 2005. Histochemical differences between motoneurons supplying multiply and singly innervated extraocular muscle fibers. *J Comp Neurol* 491:352-66.
- Edwards SB, Henkel CK. 1978. Superior colliculus connections with the extraocular motor nuclei in the cat. *J Comp Neurol* 179:451-67.
- Ericson H, Blomqvist A. 1988. Tracing of neuronal connections with cholera toxin subunit B: light and electron microscopic immunohistochemistry using monoclonal antibodies. *J Neurosci Methods* 24:225-35.
- Erichsen JT, May PJ. 2002. The pupillary and ciliary components of the cat Edinger-Westphal nucleus: a transsynaptic transport investigation. *Vis Neurosci* 19:15-29.
- Fuchs AF, Kaneko CR, Scudder CA. 1985. Brainstem control of saccadic eye movements. *Annu Rev Neurosci* 8:307-37.
- Fukushima J, Akao T, Takeichi N, Kurkin S, Kaneko CR and Fukushima K. 2005. Pursuit-Related Neurons in the Supplementary Eye Fields: Discharge During Pursuit and Passive Whole Body Rotation. *J Neurophysiol* 91, 2809-2825.
- Gamlin PDR, Reiner A, Erichsen JT, Karten HJ, Cohen DH. 1984. The neural substrate for the pupillary light reflex in the pigeon (*Columba livia*). *J Compa. Neurol* 226: 523-543.
- Gamlin PD, Gnadt JW, Mays LE. 1989. Abducens internuclear neurons carry an inappropriate signal for ocular convergence. *J Neurophysiol* 62:70-81.

- Gamlin PD, Reiner A. 1991. The Edinger-Westphal nucleus: sources of input influencing accommodation, pupilloconstriction, and choroidal blood flow. *J Comp Neurol* 306:425-38.
- Gamlin PD, Zhang Y, Clendaniel RA, Mays LE. 1994. Behavior of identified Edinger-Westphal neurons during ocular accommodation. *J Neurophysiol* 72:2368-82.
- Gamlin PD, Clarke RJ. 1995. The pupillary light reflex pathway of the primate. *J Am Optom Assoc* 66:415-8.
- Gamlin PD, Yoon K. 2000. An area for vergence eye movement in primate frontal cortex. *Nature* 407:1003-7.
- Gamlin PDR. 2005. The pretectum: connections and oculomotor-related roles. *Prog Brain Res* 151:379-405.
- Gibson AR, Hansma DI, Houk JC, Robinson FR. 1984. A sensitive low artifact TMB procedure for the demonstration of WGA-HRP in the CNS. *Brain Res* 298:235-41.
- Gonatas NK, Harper C, Mizutani T, Gonatas JO. 1979. Superior sensitivity of conjugates of horseradish peroxidase with wheat germ agglutinin for studies of retrograde axonal transport. *J Histochem Cytochem* 27:728-34.
- Gong S, LeDoux MS. 2003. Immunohistochemical detection of wheat germ agglutinin-horseradish peroxidase (WGA-HRP). *J Neurosci Methods* 126:25-34.
- Harker DW. 1972. The structure and innervation of sheep superior rectus and levator palpebrae extraocular muscles. II. Muscle Spindles. *Invest OphthalmolVis Sci* 11:970-79.
- Horn-Bochtler AK, Ardeleanu P, Messoudi A, Büttner-Ennever JA. 2006. Histochemical characteristics of cell groups in the perioculomotor area, including the Edinger-Westphal complex, in monkey and man. Poster 345.9/S4.
- Horikawa K, Powell EW. 1986. Comparison of techniques for retrograde labelling using the rat's facial nucleus. *J Neurosci Methods* 17:287-96.
- Ishikawa S, Sekiya H, Kondo Y. 1990. The center for controlling the near reflex in the midbrain of the monkey: a double labelling study. *Brain Res* 519:217-22.

- Isomura G. 1981. Comparative anatomy of the extrinsic ocular muscles in vertebrates. *Anat. Anz* 150:498-515.
- Jacoby J, Ko K, Weiss C, Rushbrook JI. 1990. Systematic variation in myosin expression along extraocular muscle fibres of the adult rat. *J Muscle Res Cell Motil* 11:25-40.
- Judge SJ, Cumming BG. 1986. Neurons in the monkey midbrain with activity related to vergence eye movement and accommodation. *J Neurophysiol* 55: 915-930.
- Kaminski HJ, Kusner LL, Block CH. 1996. Expression of acetylcholine receptor isoforms at extraocular muscle endplates. *Invest Ophthalmol Vis Sci* 37:345-51.
- Kawasaki T, Kiyosawa M, Fujino T, Tokoro T. 1993. Slow accommodation release with a cerebellar lesion. *Br J Ophthalmol* 77:678.
- Keller EL, Robinson DA. 1972. Abducens unit behavior in the monkey during vergence movements. *Vision Res* 12:369-82.
- Khanna S, Cheng G, Gong B, Mustari MJ, Porter JD. 2004. Genome-wide transcriptional profiles are consistent with functional specialization of the extraocular muscle layers. *Invest Ophthalmol Vis Sci* 45:3055-66.
- Kozicz T. 2003. Neurons colocalizing urocortin and cocaine and amphetamine-regulated transcript immunoreactivities are induced by acute lipopolysaccharide stress in the Edinger-Westphal nucleus in the rats. *Neuroscience* 116: 315-20.
- Köbber C, Thanos S. 2000. Topographic representation of the sciatic nerve motor neurons in the spinal cord of the adult rat correlates to region-specific activation patterns of microglia. *J Neurocytol* 29:271-83.
- Krug K, Smith AL, Thompson ID. 1998. The development of topography in the hamster geniculo-cortical projection. *J Neurosci* 18:5766-76.
- Leman S, Viltart O, Sequeira H. 2000. Double immunocytochemistry for the detection of Fos protein in retrogradely identified neurons using cholera toxin B subunit. *Brain Res Brain Res Protoc* 5:298-304.

Leigh RJ and Zee DS. 1999. The neurology of eye movements. Oxford University Press, New York.

Leigh RJ and Zee DS. 2006. The neurology of eye movements. Oxford University Press, New York.

Lippincott Williams & Wilkins. 2005. Porth's Pathophysiology: concept of altered health states. Seventh Edition.

Llewellyn-Smith IJ, Phend KD, Minson JB, Pilowsky PM, Chalmers JP. 1992. Glutamate-immunoreactive synapses on retrogradely-labelled sympathetic preganglionic neurons in rat thoracic spinal cord. *Brain Res* 581:67-80.

Loewy AD, Saper CB. 1978. Edinger-Westphal nucleus: projection to the brain stem and spinal cord in the cat. *Brain Res* 150: 1-27.

Luppi PH, Fort P, Jouviet M. 1990. Iontophoretic application of unconjugated cholera toxin B subunit (CTB) combined with immunohistochemistry of neurochemical substances: a method for transmitter identification of retrogradely labeled neurons. *Brain Res* 534:209-24.

Lukas JR, Blumer R, Denk M, Baumgartner I, Neuhuber W, Mayr R. 2000. Innervated myotendinous cylinders in human extraocular muscles. *Invest Ophthalmol Vis Sci* 41:2422-31.

Lyman D, E. Mugnaini. 1980. The avian accessory oculomotor nucleus. *Soc. Neurosci. Abstr.* 6; 479.

Maciewicz R, Phipps BS, Foote WE, Aronin N, DiFiglia M. 1983. The distribution of substance P-containing neurons in the cat Edinger-Westphal nucleus: relationship to efferent projection systems. *Brain Res* 270:217-30.

May PJ, Porter JD, Gamlin PD. 1992. Interconnections between the primate cerebellum and midbrain near-response regions. *J Comp Neurol* 315:98-116.

May P J, Wright NF, Lin RC-S. and Erichsen J.T.. 2000. Light and electron microscopic features of medial rectus C-subgroup motoneurons in macaques suggest near triad specialization. *Invest. Ophthalm. and Vis. Sci.* 41: S820.

- Mayr R, Gottschall J, Gruber H, Neuhuber W. 1975. Internal structure of cat extraocular muscle. *Anat Embryol (Berl)* 148:25-34.
- Mays LE. 1984. Neural control of vergence eye movement: convergence and divergence neurons in the midbrain. *J Neurophysiol* 51: 1091-1108.
- Mays LE, Porter JD. 1984. Neural control of vergence eye movements: activity of abducens and oculomotor neurons. *J Neurophysiol* 52:743-61.
- McLoon LK, Wirtschafter JD. 1996. N-CAM is expressed in mature extraocular muscles in a pattern conserved among three species. *Invest Ophthalmol Vis Sci* 37:318-27.
- Mesulam MM. 1978. Tetramethyl benzidine for horseradish peroxidase neurohistochemistry: a non-carcinogenic blue reaction product with superior sensitivity for visualizing neural afferents and efferents. *J Histochem Cytochem* 26:106-17.
- Mesulam MM, Mufson EJ. 1980. The rapid anterograde transport of horseradish peroxidase. *Neuroscience* 5:1277-86.
- Mesulam, M.M. 1982. *Tracing Neural Connections with Horseradish Peroxidase*, Wiley, New York.
- Miller JM, Bockisch CJ, Pavlovski DS. 2002. Missing lateral rectus force and absence of medial rectus co-contraction in ocular convergence. *J Neurophysiol* 87: 2421-2433.
- Moore GE, Schachat FH. 1985. Molecular heterogeneity of histochemical fibre types: a comparison of fast fibres. *J Muscle Res Cell Motil* 6:513-24.
- Morgan DL, Proske U. 1984. Vertebrate slow muscle: its structure, pattern of innervation, and mechanical properties. *Physiol Rev* 64:103-69.
- Nakao S, Shiraishi Y, Miyara T. 1986. Direct projection of cat midbrain tegmentum neurons to the medial rectus subdivision of the oculomotor complex. *Neurosci Lett* 64:123-8.
- Narayanan CH, Narayanan Y. 1976. An experimental inquiry into the central source of preganglionic fibers to the chick ciliary ganglion. *J Comp Neurol* 166:101-9.

- Oh SY, Poukens V, Demer JL. 2001. Quantitative analysis of rectus extraocular muscle layers in monkey and humans. *Invest Ophthalmol Vis Sci* 42:10-6.
- Pachter BR. 1983. Rat extraocular muscle. 1. Three dimensional cytoarchitecture, component fibre populations and innervation. *J Anat* 137:143-59.
- Pachter BR, Colbjornsen C. 1983. Rat extraocular muscle. 2. Histochemical fibre types. *J Anat* 137:161-70.
- Peyron C, Petit JM, Rampon C, Jouvet M, Luppi PH. 1998. Forebrain afferents to the rat dorsal raphe nucleus demonstrated by retrograde and anterograde tracing methods. *Neuroscience* 82:443-68.
- Pierobon-Bormioli S, Sartore S, Libera LD, Vitadello M, Schiaffino S. 1981. "Fast" isomyosins and fiber types in mammalian skeletal muscle. *J Histochem Cytochem* 29: 1179-88.
- Porter JD, Baker RS, Ragusa RJ, Brueckner JK. 1995. Extraocular muscles: basic and clinical aspects of structure and function. *Surv Ophthalmol* 39:451-84.
- Reiner A, Karten HJ, Gamlin PDR and Erichsen JT. 1983. Parasympathetic ocular control: functional subdivisions and circuitry of the avian nucleus of Edinger-Westphal. *Trends Neurosci* 6: 140-145.
- Richmond FJ, Johnston WSW, Baker RS, Steinbach MJ. 1984. Palisade endings in human extraocular muscle. *Invest Ophthalmol Vis Sci* 25:471-476.
- Robinson DA. 1970. Oculomotor unit behavior in the monkey. *J Neurophysiol* 33: 393-403.
- Ruda M, Coulter JD. 1982. Axonal and transneuronal transport of wheat germ agglutinin demonstrated by immunocytochemistry. *Brain Res* 249:237-46.
- Ruskell GL. 1978. The fine structure of innervated myotendinous cylinders in extraocular muscles of rhesus monkeys. *J Neurocytol* 7:693-708.
- Ruskell GL. 1999. Extraocular muscle proprioceptors and proprioception. *Prog Retin Eye Res* 18:269-91.

Schiaffino S, Hanzlikova V, Pierobon S. 1970. Relations between structure and function in rat skeletal muscle fibers. *J Cell Biol* 47:107-19.

Schünke M, Schulte E, Schumacher U. 2006. Prometheus Lernatlas der Anatomie. P135.

Sevel D. 1986. The origins and insertions of the extraocular muscles: development, histologic features, and clinical significance. *Trans Am Ophthalmol Soc* 84:488-526.

Shall MS, Dimitrova DM, Goldberg SJ. 2003. Extraocular motor unit and whole-muscle contractile properties in the squirrel monkey. Summation of forces and fiber morphology. *Exp Brain Res* 151:338-45.

Shaw MD, Alley KE. 1981. Generation of the ocular motor nuclei and their cell types in the rabbit. *J Comp Neurol* 200:69-82.

Shook BL, Schlag-Rey M, Schlag J. 1990. Primate supplementary eye field: I. Comparative aspects of mesencephalic and pontine connections. *J Comp Neurol* 301:618-42.

Siebeck R, Krüger P. 1955. The histological structure of the extrinsic ocular muscles as an indication of their function. *Albrecht Von Graefes Arch Ophthalmol* 156:636-52.

Spencer RF, Porter JD. 1981. Innervation and structure of extraocular muscles in the monkey in comparison to those of the cat. *J Comp Neurol* 198:649-65.

Spencer RF, Porter JD. 1988. Structural organization of the extraocular muscles. *Rev Oculomot Res* 2:33-79.

Spencer RF, Porter JD. 2006. Biological organization of the extraocular muscles. *Prog Brain Res* 151:43-80.

Spina MG, Langnaese K, Orlando GF, Horn TF, Rivier J, Vale WW, Wolf G, Engelmann M. 2004. Colocalization of urocortin and neuronal nitric oxide synthase in the hypothalamus and Edinger-Westphal nucleus of the rat. *J Comp Neurol* 479:271-86.

Stanton GB, Goldberg ME, Bruce CJ. 1988. Frontal eye field efferents in the macaque monkey: II. Topography of terminal fields in midbrain and pons. *J Comp Neurol* 271:493-506.

Strassman A, Mason P, Eckenstein F, Baughman RW, Maciewicz R. 1987. Choline acetyltransferase immunocytochemistry of Edinger-Westphal and ciliary ganglion afferent neurons in the cat. *Brain Res* 423: 293-304.

Sugimoto T, Itoh K, Mizuno N. 1977. Localization of neurons giving rise to the oculomotor parasympathetic outflow: an HRP study in cat. *Neurosci.Letter* 7: 301-305.

Sun W, May PJ. 1993. Organization of the extraocular and preganglionic motoneurons supplying the orbit in the lesser Galago. *Anat Rec* 237:89-103.

Teune TM, van der Burg J, de Zeeuw CI, Voogd J, Ruigrok TJ. 1998. Single Purkinje cell can innervate multiple classes of projection neurons in the cerebellar nuclei of the rat: a light microscopic and ultrastructural triple-tracer study in the rat. *J Comp Neurol* 392:164-78.

Toyoshina K, Kawana E, Sakai H. 1980. On the neuronal origin of the afferents to the ciliary ganglion in cat. *Brain Res.* 185: 67-76.

Trott JR, Apps R. 1993. Zonal organization within the projection from the inferior olive to the rostral paramedian lobule of the cat cerebellum. *Eur J Neurosci* 5:162-73.

Ugolini G, Klam F, Doldan Dans M, Dubayle D, Brandi AM, Büttner-Ennever J, Graf W. 2006. Horizontal eye movement networks in primates as revealed by retrograde transneuronal transfer of rabies virus: differences in monosynaptic input to "slow" and "fast" abducens motoneurons. *J Comp Neurol* 498:762-85.

Wasicky R, Ziya-Ghazvini F, Blumer R, Lukas JR, Mayr R. 2000. Muscle fiber types of human extraocular muscles: a histochemical and immunohistochemical study. *Invest Ophthalmol Vis Sci* 41:980-90.

Wasicky R, Horn AK, Büttner-Ennever JA. 2004. Twitch and non-twitch motoneuron subgroups in the oculomotor nucleus of monkeys receive different afferent projections. *J Comp Neurol* 479:117-29.

Wieczorek DF, Periasamy M, Butler-Browne GS, Whalen RG, Nadal-Ginard B. 1985. Co-expression of multiple myosin heavy chain genes, in addition to a tissue-specific one, in extraocular musculature. *J Cell Biol* 101:618-29.

Zhang H, Gamlin PD. 1998. Neurons in the posterior interposed nucleus of the cerebellum related to vergence and accommodation. I. Steady-state characteristics. *J Neurophysiol* 79 :1255-69.

Zhang Y, Gamlin PD, Mays LE. 1991. Antidromic identification of midbrain near response cells projecting to the oculomotor nucleus. *Exp Brain Res* 84:525-8.

Zhang Y, Mays LE, Gamlin PD. 1992. Characteristics of near response cells projecting to the oculomotor nucleus. *J Neurophysiol* 67:944-60.

7 Attachment

WGA-HRP immunocytochemical labelling

TMB-Reaction

- washed the sections in cold 0.1M PBS, pH 7.4
- washed the sections in cold aqua bidest, 3x1min
- pretreated the sections with solution which contains solution A+B, 20min
 - solution A:** 370 ml aqua bidest + 20 ml Na-Acetabuffer pH 3.3
+400 mg Sodium-Nitroferroprussiat (Na-Nitroprusside dihydrate)
 - solution B:** 10 ml, 100% Ethanol + 20 mg Tetramethylbenzidine staining
- washed the sections in 50 ml Acetate buffer + 950 ml aqua bidest. , 2x5min
- stabilized the section in 20 g Ammoniumheptamolybdat in 400 ml aqua bidest, 20min
- washed the sections in 0,1M PBS, 30 sec
- incubated the sections into the solution (120µl 30% H₂O₂ into DAB-Co-solution), 5-8 min
 - solution A:** 200 mg Diaminobenzidine in 200 ml aqua bidest solution + 200 ml 0.2M PBS, pH 7.4
 - solution B:** 80 mg Co-Chlorid in 8 ml aqua. Bidest solution (1% solution)
- washed the sections in 0.1M PBS, 3x 1min

Cholera toxin subunit B immunocytochemical labelling

- shortly washed the sections in 0.1M PBS, pH 7.4
- pretreated the sections with 10% methanol/3% H₂O₂ 15 min to suppress endogenous peroxidase activity
- washed the sections in 0.1M PBS, pH 7.4, 3x10 min
- blocked with 5% normal rabbit serum in 0.1M PBS, pH 7.4 containing 0.3% Triton for 1hour room temperature
- incubated with goat choleraenoid antibody (1: 20,000) for 48 hours at 4° C
- washed the section in 0.1M PBS, pH 7.4, 3x10 min
- incubated with second antibody rabbit anti-goat 1:200 (50µl in 10 ml PBS pH 7.4) 1hour room temperature
- washed the sections in 0.1M PBS, pH 7.4, 3x10 min
- EAP Extravidin-Peroxidase 1:1000 (10µl in 10 ml) 1hour room temperature

- washed the sections in 0.1M PBS, pH 7.4, 2x10min
- washed the sections in 0.1M TBS, pH 7.6, 1x10min
- Diaminobenzidine reaction 10min
 - 0.05% DAB +0.01% H₂O₂ in 0.05 M TBS, pH8
- washed the sections in 0.1M PBS, pH 7.4, 3x10min
- dried the section in room temperature and covered the slices

Nissl staining

Solution: 0.5g cresyl violet in 100ml distilled water

- dehydrate:
 - 70% alcohol for 5 min
 - 90% alcohol for 5 min
 - 96% alcohol I for 5 min
 - 100% alcohol for 5 min
 - Xylene for 15 min
 - Xylene for 15 min
- rehydrate and stain:
 - 100% alcohol for 5 min
 - 96% alcohol for 5 min
 - 90% alcohol for 5 min
 - 70% alcohol for 5 min
- distilled water 5 min
- 0.5% cresyl violet solution for 5 min
- shortly washed the sections in distilled Water
- dehydrate:
 - 70% alcohol for 5 min
 - 90% alcohol for 5 min
 - 96% alcohol I for 5 min
 - 100% alcohol for 5 min
 - Xylene for 15 min
 - Xylene for 15 min
- coverslip
- leave the slides at room temperature for drying.

8 Acknowledgements



I would like to thank my supervisor, Prof. Dr. Jean Büttner-Ennever for giving the opportunity of doing my doktorarbeit in her group, for her invaluable support and kindness, and excellent environment and the motivation she created for me.

I wish to express my gratitude to PD. Dr. Anja K. Horn-Bochtler for giving valuable suggestions during the experiment and discussing the thesis together.

In particular, I am also very grateful to Prof. Dr. med. Ulrich Büttner for his constant encouragement, valuable suggestions, critical reading of the manuscript and financial supporting.

Essential support in the experiments has been given by A. Messoudi, MPhil; MLS., who answered me so many questions about the staining throughout my research.

Special thanks to Rita Büttner, Karoline Fackelmann, Christina Schulze and Christine Glombik for the happiest time we spent together in the lab.

Finally I would like to thank my family and my teachers in China for their love and great support, as well as all of my friends for their friendship and consideration through my Dr. med.

9 Curriculum Vitae

Personal data

| | |
|----------------|---|
| Name | Xiaofang Tang |
| Gender | Female |
| Date of Birth | July 4, 1978 |
| Place of Birth | Weihai city, Shandong Province, P. R. China |
| Citizenship | P. R. China |

Education history:

| | |
|--------------|---|
| 2006-Present | Institute of Anatomy, Ludwig-Maximilians-Universität München |
| 2004-2006 | Department of Neurology, Ludwig-Maximilians-Universität München |
| 2001-2004 | Qingdao University, Medical College Qingdao, Shandong Master of Physiology |
| 1999-2001 | Jining Medical College Jining, Shandong Bachelor of Clinical Medicine |
| 1996-1999 | Heze Medical Academy Heze, Shandong |

Scholarship and honors:

| | |
|-----------|--|
| 1999-2001 | awarded the first prize for the outstanding student twice in Jijing Medical College |
| 1999.7 | graduate with the honor of “Excellent High educated-Graduate of Shandong Province” in Heze Medical Academy |
| 1996-1999 | as an outstanding student in the whole school won the first scholarship in Heze Medical Academy |

Research work:

| | |
|----------------|---|
| 2006.1-2006.12 | Perform the immunohistochemical experiment to check the location of C-group motoneurons in the monkey and their dendritic spread by simultaneously injection WGA-HRP and CTB into the distal tip of the eye muscles. |
| 2004.7-2005.12 | Record extracellularly from single neuron in the fastigial oculomotor region by tungsten electrode during the monkey performed the visually guided small saccades. |
| 2001.9-2004.6 | Perform electrophysiological experiments with multiple-microelectrode extracellularly recording technique; to check the expression of neuro-peptide-containing cells in brain; by the microinjection on rats by the immunohistochemical technique; to check the volume of food intake. The work was as a part of the research for the central effect of ghrelin on the regulation of gastric motility in the rat. |